Precision neutrino oscillation physics with an intermediate baseline reactor neutrino experiment

Sandhya Choubey
INFN, Sezione di Trieste, Trieste, Italy
and Scuola Internazionale Superiore di Studi Avanzati, I-34014 Trieste, Italy

S. T. Petcov
Scuola Internazionale Superiore di Studi Avanzati, I-34014 Trieste, Italy,
INFN, Sezione di Trieste, Trieste, Italy,
and Institute of Nuclear Research and Nuclear Energy, Bulgarian Academy of Sciences, 1784 Sofia, Bulgaria

M. Piai
Department of Physics, Yale University, New Haven, Connecticut 06520, USA
(Received 16 June 2003; published 30 December 2003)

We discuss the physics potential of intermediate $L\sim 20$–30 km baseline experiments at reactor facilities. Assuming that the solar neutrino oscillation parameters $\Delta m^2_{\odot}$ and $\theta_{\odot}$ lie in the high LMA solution region, we show that such an intermediate baseline reactor experiment can determine both $\Delta m^2_{\odot}$ and $\theta_{\odot}$ with a remarkably high precision. We perform also a detailed study of the sensitivity of the indicated experiment to $\Delta m^2_{\rm atm}$, which drives the dominant atmospheric ν_μ ($\overline{\nu}_\mu$) oscillations, and to θ—the neutrino mixing angle limited by the data from the CHOOZ and Palo Verde experiments. Irrespective of the actual values of $\Delta m^2_{\odot}$, we find that this experiment can improve the bounds on $\sin^2\theta$, and, if the value of $\sin^2\theta$ is large enough, $\sin^2\theta \gtrsim 0.02$, the energy resolution of the detector is sufficiently good and if the statistics is relatively high, it can determine with extremely high precision the value of $\Delta m^2_{\rm atm}$. We also explore the potential of the intermediate baseline reactor neutrino experiment for determining the type of the neutrino mass spectrum, which can be with normal or inverted hierarchy, assuming $\Delta m^2_{\odot}$ to lie in the high LMA solution region. We show that the conditions under which the type of neutrino mass hierarchy can be determined are quite challenging, but are within the reach of the experiment under discussion.

DOI: 10.1103/PhysRevD.68.113006 PACS number(s): 14.60.Pq, 13.15.+g

I. INTRODUCTION

The experiments with solar, atmospheric and reactor neutrinos [1–6] have provided in recent years remarkable evidence for the existence of neutrino oscillations driven by nonzero neutrino masses and neutrino mixing. The hypothesis of solar neutrino oscillations, which in one variety or another were considered as the most natural explanation of the solar neutrino deficit [1,2] since the late 1960s (see, e.g., [7–9]), has received a convincing confirmation from the measurement of the solar neutrino flux through the neutral current reaction on deuterium by the SNO experiment [3]. The analysis of the solar neutrino data obtained by Homestake, SAGE, GALLEX/GNO, SK and SNO experiments showed that the data favor the large mixing angle (LMA) Mikheyev-Smirnov-Wolfenstein (MSW) solution with the two-neutrino oscillation parameters—the solar neutrino mixing angle and the mass squared difference, lying at 99.73% C.L. in the region [3,10]:

$$3\times 10^{-5}\ \ \mathrm{eV}^2 \lesssim \Delta m^2_{\odot} \lesssim 3.5\times 10^{-4}\ \ \mathrm{eV}^2, \tag{1}$$

$$0.21 \lesssim \sin^2\theta_{\odot} \lesssim 0.47. \tag{2}$$

The first results of the KamLAND reactor experiment [6] has confirmed, under the plausible assumption of *CPT* invariance which we will suppose to hold throughout this study, the LMA MSW solution, establishing it essentially as a unique solution of the solar neutrino problem. The combined fits to the available solar neutrino and KamLAND data, performed by several collaborations within the two-neutrino mixing hypothesis, identify two distinct solution subregions within the LMA solution region [11–13]. Adding the KamLAND data did not lead to a considerable reduction of the interval of allowed values of $\sin^2\theta_{\odot}$ with respect to the one quoted in Eq. (1), while the best fit values of $\Delta m^2_{\odot}$ in the two sub-regions (labeled from now on low LMA and high LMA) are given by [12]

$$\text{low LMA:}\ \ \Delta m^2_{\odot} \simeq 7.2\times 10^{-5}\ \ \mathrm{eV}^2, \tag{3}$$

$$\text{high LMA:}\ \ \Delta m^2_{\odot} \simeq 1.5\times 10^{-4}\ \ \mathrm{eV}^2. \tag{4}$$

The observed Zenith angle dependence of the multi-GeV μ-like events in the Super-Kamiokande experiment unambiguously demonstrated the disappearance of the atmospheric ν_μ ($\overline{\nu}_\mu$) on distances $L \gtrsim 1000$ km. The Super-Kamiokande (SK) atmospheric neutrino data is best described, as is well known, in terms of dominant $\nu_\mu \to \nu_\tau$ ($\overline{\nu}_\mu \to \overline{\nu}_\tau$) oscillations with (almost) maximal mixing and neutrino mass squared difference of $|\Delta m^2_{\rm atm}| \cong (1.4-5.0)\times 10^{-3}$ eV^2 (99.73% C.L.) [4]. According to the more recent combined analysis of the data from the SK and K2K experiments [14] one has at 99.73% C.L.:

 ©2003 The American Physical Society

$$1.5\times10^{-3}\ \text{eV}^2 \lesssim |\Delta m^2_{\text{atm}}| \lesssim 3.7\times10^{-3}\ \text{eV}^2. \tag{5}$$

The neutrino oscillation description of the combined solar and atmospheric neutrino data requires the existence of three-neutrino mixing in the weak charged lepton current (see, e.g., [15]):

$$\nu_{l\text{L}} = \sum_{j=1}^{3} U_{lj}\nu_{j\text{L}}. \tag{6}$$

Here ν_{lL}, $l=e,\mu,\tau$, are the three left-handed flavor neutrino fields, $\nu_{j\text{L}}$ is the left-handed field of the neutrino ν_j having a mass m_j and U is the Pontecorvo-Maki-Nakagawa-Sakata (PMNS) neutrino mixing matrix [16,17]. The PMNS mixing matrix U can be parametrized by three angles, θ_{atm}, $\theta_\odot$, and θ, and, depending on whether the massive neutrinos ν_j are Dirac or Majorana particles—by one or three *CP*-violating phases [18,19]. In the standard parametrization of U (see, e.g., [15]) the three mixing angles are denoted as θ_{12}, θ_{13} and θ_{23}:

$$U = \begin{pmatrix} U_{e1} & U_{e2} & U_{e3} \\ U_{\mu1} & U_{\mu2} & U_{\mu3} \\ U_{\tau1} & U_{\tau2} & U_{\tau3} \end{pmatrix} = \begin{pmatrix} c_{12}c_{13} & s_{12}c_{13} & s_{13}e^{-i\delta} \\ -s_{12}c_{23}-c_{12}s_{23}s_{13}e^{i\delta} & c_{12}c_{23}-s_{12}s_{23}s_{13}e^{i\delta} & s_{23}c_{13} \\ s_{12}s_{23}-c_{12}c_{23}s_{13}e^{i\delta} & -c_{12}s_{23}-s_{12}c_{23}s_{13}e^{i\delta} & c_{23}c_{13} \end{pmatrix}, \tag{7}$$

where we have used the usual notations, $s_{ij}\equiv\sin\theta_{ij}$, $c_{ij}\equiv\cos\theta_{ij}$, and δ is the Dirac *CP*-violation phase.[1] If we identify the two independent neutrino mass squared differences in this case, Δm^2_{21} and Δm^2_{31}, with the neutrino mass squared differences which drive the solar and atmospheric neutrino oscillations, $\Delta m^2_\odot = \Delta m^2_{21} > 0$, $\Delta m^2_{\text{atm}} = \Delta m^2_{31}$, one has $\theta_{12} = \theta_\odot$, $\theta_{23} = \theta_{\text{atm}}$, and $\theta_{13} = \theta$.

The angle θ is limited by the data from the CHOOZ and Palo Verde experiments [21,22] which searched for evidences for oscillations of reactor $\bar{\nu}_e$ at $\sim$1 km from the source. No disappearance of $\bar{\nu}_e$ was observed. In a two-neutrino oscillation analysis performed in [21] a stringent upper bound on the value of θ in the region of $|\Delta m^2| \geqslant 1.5\times10^{-3}$ eV^2 was obtained. A 3-ν oscillation analysis of the CHOOZ data[2] [23] led to the conclusion that for $\Delta m^2_\odot \lesssim 10^{-4}$ eV^2, the limits on $\sin^2\theta$ practically coincide with those derived in the 2-ν oscillation analysis in [21]. A combined 3-ν oscillation analysis of the solar neutrino, CHOOZ and the KamLAND data, performed under the assumption of $\Delta m^2_\odot \ll |\Delta m^2_{\text{atm}}|$ (see, e.g., [15,24]), showed that [11]

$$\sin^2\theta < 0.05, \quad 99.73\%\ \text{C.L.} \tag{8}$$

The precise upper limit in Eq. (8) is Δm^2_{atm} dependent. The authors of [11] found the best-fit value of $\sin^2\theta$ to lie in the interval[3] $\sin^2\theta \cong (0.00-0.01)$.

Somewhat better limits on $\sin^2\theta$ than the existing one can be obtained in the MINOS experiment [26]. Various options are being currently discussed (experiments with off-axis neutrino beams, more precise reactor antineutrino and long baseline experiments, etc., see, e.g., [27]) of how to improve by at least an order of magnitude, i.e., to values of $\sim$0.005 or smaller, the sensitivity to $\sin^2\theta$.

Let us note that the atmospheric neutrino and K2K data do not allow one to determine the sign of Δm^2_{atm}. This implies that if we identify Δm^2_{atm} with Δm^2_{31} in the case of 3-neutrino mixing, one can have $\Delta m^2_{31} > 0$ or $\Delta m^2_{31} < 0$. The two possibilities correspond to two different types of neutrino mass spectrum: with normal hierarchy (NH), $m_1 < m_2 < m_3$, and with inverted hierarchy (IH), $m_3 < m_1 < m_2$.

After the spectacular experimental progress made in the last two years or so in the studies of neutrino oscillations, further understanding, in particular, of the structure of the neutrino masses and mixing, of their origins and of the status of the *CP*-symmetry in the lepton sector requires a large and challenging program of high precision measurements to be pursued in neutrino physics. One of the first goals of this program is to improve the precision in the measurement of the mass squared differences and mixing angles which control the solar and the dominant atmospheric neutrino oscillations: $\Delta m^2_\odot$, $\theta_\odot$, and Δm^2_{atm}, θ_{atm}. A step of fundamental importance would be the detection and the studies of subleading neutrino oscillation effects, if the latter are observable. This includes the measurement of, or getting more stringent upper limit on, the value of the third and the only small mixing angle in the PMNS matrix U, θ $(=\theta_{13})$, the exploration of the possible *CP*-violating effects and the determination of the type of the neutrino mass spectrum which can be with normal hierarchy (NH) or inverted hierarchy (IH). Among the further fundamental open questions, which cannot be answered by studying neutrino oscillations, but the progress in the studies of which requires a precise knowledge of the neutrino oscillation parameters, are (i) the nature—

[1]We have not written explicitly the two possible Majorana *CP*-violation phases [18,19] which do not enter into the expressions for the oscillation probabilities of interest [18,20]. We assume throughout this study $0 \leqslant \theta_{12}, \theta_{23}, \theta_{13} < \pi/2$.

[2]In this case $\Delta m^2 = \Delta m^2_{\text{atm}}$.

[3]The possibility of large $\sin^2\theta > 0.97$, which is admitted by the CHOOZ data alone, is incompatible with the neutrino oscillation interpretation of the solar neutrino data (see, e.g., [25]).

Dirac or Majorana—of the massive neutrinos, (ii) the absolute scale of neutrino masses, (iii) the mechanism giving rise to the neutrino masses and mixing, (iv) the possible relation between *CP* violation in the lepton sector at low energies and the generation of the baryon asymmetry of the Universe by the leptogenesis mechanism, and (v) lepton number violation and its possible manifestation in charged lepton flavor violating decays, to name a few.

In the present article we explore the possibility of performing a high precision measurement of some of the 3-neutrino oscillation parameters in an intermediate baseline, $L\sim 20$–30 km, reactor neutrino experiment. We first address the issue of precision determination of the solar neutrino oscillation parameters, $\Delta m^2_\odot$ and $\theta_\odot$. The KamLAND experiment, as discussed by several authors [28], has a remarkable sensitivity to $\Delta m^2_\odot$ in the low LMA region. However, the sensitivity of KamLAND to the value of $\theta_\odot$ is not found to be equally good. Even under the most optimistic conditions KamLAND is not expected to substantially reduce the region of allowed values of $\theta_\odot$ obtained from the analysis of the solar neutrino data [29]. The best conditions for precise determination of $\theta_\odot$ is in a reactor experimental setup, where the baseline is tuned to a Survival Probability MINimum (SPMIN).[4] With a baseline of about $L\sim 160$ km and $\Delta m^2_\odot \sim 7.2\times 10^{-5}$ eV^2 or 1.5×10^{-4} eV^2, KamLAND is essentially sensitive to a Survival Probability MAXimum (SPMAX). The sensitivity to SPMAX gives KamLAND the ability to determine $\Delta m^2_\odot$ with a high precision through the measurement of the distortion of the final state e^+ spectrum, provided $\Delta m^2_\odot < 2\times 10^{-4}$ eV^2. At the same time it reduces KamLAND's sensitivity to the solar neutrino mixing angle [29]. As was shown in [29], a 70 km baseline reactor experiment could determine the solar neutrino mixing angle $\sin^2\theta_\odot$ ($\tan^2\theta_\odot$) to within 9.6 (14)% at the 99% C.L. in the case of the low LMA solution of the solar neutrino problem. KamLAND essentially looses sensitivity to $\Delta m^2_\odot$ for $\Delta m^2_\odot \gtrsim 2\times 10^{-4}$ eV^2. Nevertheless, the more precise measurement of the spectrum of the final state e^+ in the KamLAND experiment is expected to unambiguously determine whether $\Delta m^2_\odot$ lies in the low LMA or high LMA region.

In this paper, following a previous suggestion and analysis in [30] (see also [31]), in the context of three neutrino mixing, we discuss the physics potential of intermediate $L\sim 20$–30 km baseline experiments at reactor facilities. We show that such an intermediate baseline reactor experiment can determine both $\Delta m^2_\odot$ and $\theta_\odot$ with a remarkably high precision *if the solution of the solar neutrino problem is the high LMA solution*. We perform also a detailed study of the sensitivity of the indicated experiment to the parameters $\Delta m^2_{\rm atm}$ and $\sin^2\theta$. We show that if the energy resolution of the detector is sufficiently good and if the statistics is relatively high, one can choose small enough energy bins so that even an experiment with an intermediate baseline of 20–30 km can be sensitive to the $\Delta m^2_{\rm atm}$ driven oscillations. We find that this experiment can certainly improve the bounds on $\sin^2\theta$ and if the value of $\sin^2\theta$ is large enough, it can determine with extremely high precision the value of $\Delta m^2_{\rm atm}$.

We finally explore the potential of the intermediate baseline reactor neutrino experiment for determining the type of the neutrino mass spectrum which can be with normal or inverted hierarchy. The knowledge of the neutrino mass hierarchy is of crucial importance, in particular, for modeling of the neutrino mass matrix and understanding of the underlying physics of neutrino mass generation. The type of the neutrino mass hierarchy has been also shown to be an important "parameter" in a number of neutrino mixing and neutrino oscillation observables, such as the effective Majorana mass in neutrinoless double-β decay [32]. The neutrino mass hierarchy (or, e.g., the sign of $\Delta m^2_{\rm atm}$) can be determined in very long baseline neutrino oscillation experiments at neutrino factories (see, e.g., [33]), and, e.g, using combined data from the long baseline oscillation experiments JHF-SK and NuMI with off-axis neutrino beams [34]. It was suggested in [30] that the "interference" effects between the $\Delta m^2_\odot$ and $\Delta m^2_{\rm atm}$ driven oscillations can be used in reactor experiments to answer the question about the neutrino mass hierarchy. We show that the conditions under which the type of neutrino mass hierarchy can be determined are rather challenging, but are not out of reach of the experiment under discussion, provided the solar neutrino oscillation parameters lie in the high-LMA solution region.

II. THE THREE-GENERATION $\overline{\nu}_E$ SURVIVAL PROBABILITY

The expression for the $\overline{\nu}_e$ survival probability in the case of 3 flavor neutrino mixing and neutrino mass spectrum with normal hierarchy (NH) is given by[5] [23,30,35]

$$\begin{aligned} P_{NH}(\overline{\nu}_e\to\overline{\nu}_e) = {} & 1-2\sin^2\theta\cos^2\theta\left(1-\cos\frac{\Delta m^2_{\rm atm}L}{2E_\nu}\right) \\ & -\frac{1}{2}\cos^4\theta\sin^2 2\theta_\odot\left(1-\cos\frac{\Delta m^2_\odot L}{2E_\nu}\right) \\ & +2\sin^2\theta\cos^2\theta\sin^2\theta_\odot \\ & \times\left(\cos\left(\frac{\Delta m^2_{\rm atm}L}{2E_\nu}-\frac{\Delta m^2_\odot L}{2E_\nu}\right)-\cos\frac{\Delta m^2_{\rm atm}L}{2E_\nu}\right), \end{aligned} \tag{9}$$

where E_ν is the $\overline{\nu}_e$ energy. If the neutrino mass spectrum is with inverted hierarchy (IH), the $\overline{\nu}_e$ survival probability can be written in the form [23,30,35]

[4]A detailed discussion of SPMAX and SPMIN as well as $\theta_\odot$ sensitivity of the current and future experiments can be found in [29] and we do not repeat it here.

[5]The Earth matter effects are negligible for the values of the neutrino oscillation parameters ($\Delta m^2_\odot$ and $\Delta m^2_{\rm atm}$), $\overline{\nu}_e$ energies and the short baseline $L\simeq 20$–30 km we are interested in.

$$P_{IH}(\bar{\nu}_e \to \bar{\nu}_e) = 1 - 2\sin^2\theta\cos^2\theta\left(1 - \cos\frac{\Delta m^2_{\rm atm} L}{2E_\nu}\right) - \frac{1}{2}\cos^4\theta\sin^2 2\theta_\odot\left(1 - \cos\frac{\Delta m^2_\odot L}{2E_\nu}\right) + 2\sin^2\theta\cos^2\theta\cos^2\theta_\odot \times\left(\cos\left(\frac{\Delta m^2_{\rm atm} L}{2E_\nu} - \frac{\Delta m^2_\odot L}{2E_\nu}\right) - \cos\frac{\Delta m^2_{\rm atm} L}{2E_\nu}\right). \tag{10}$$

The $\bar{\nu}_e$ survival probability does not depend either on the angle θ_{atm} associated with the atmospheric neutrino oscillations, nor on the *CP* violating phase δ in the PMNS matrix.

In the convention (we will call A) in which the neutrino masses are not ordered in magnitude and the NH neutrino mass spectrum corresponds to $m_1 < m_2 < m_3$, while the IH spectrum is associated with the ordering $m_3 < m_1 < m_2$, it is natural to choose

$$\Delta m^2_\odot = \Delta m^2_{21} > 0, \quad \text{convention A.} \tag{11}$$

We can identify further $\Delta m^2_{\rm atm}$ with Δm^2_{31} in the case of NH spectrum,

$$\Delta m^2_{\rm atm} = \Delta m^2_{31} > 0, \quad \text{NH spectrum (A)}, \tag{12}$$

and with $\Delta m^2_{23} > 0$ if the spectrum is of the IH type,

$$\Delta m^2_{\rm atm} = \Delta m^2_{23} > 0, \quad \text{IH spectrum (A)}. \tag{13}$$

In this convention the mixing angles in the standard parametrization of the PMNS mixing matrix U are given by

$$\theta_{12} = \theta_\odot, \quad \theta_{23} = \theta_{\rm atm}, \quad \theta_{13} = \theta, \quad \text{convention A.} \tag{14}$$

One can also number (without loss of generality) the neutrinos with definite mass in vacuum ν_j in such a way that their masses obey $m_1 < m_2 < m_3$. In this alternative convention (we will denote as B) it is convenient to choose

$$\Delta m^2_{\rm atm} = \Delta m^2_{31} > 0, \quad \text{convention B.} \tag{15}$$

In the case of NH neutrino mass spectrum we have

$$\Delta m^2_\odot = \Delta m^2_{21} > 0, \quad \text{NH spectrum (B)}, \tag{16}$$

and

$$\theta_{12} = \theta_\odot, \quad \theta_{23} = \theta_{\rm atm}, \quad \theta_{13} = \theta, \quad \text{NH spectrum (B)}, \tag{17}$$

where θ_{ij} are the angles in the standard parametrization of U, Eq. (7).

If the neutrino mass spectrum is with IH, one has in this convention (see, e.g., [32,36])

$$\Delta m^2_\odot = \Delta m^2_{32} > 0, \quad \text{IH spectrum (B)}, \tag{18}$$

and

$$|U_{e2}| = \cos\theta_\odot\sqrt{1 - |U_{e1}|^2},$$
$$|U_{e3}| = \sin\theta_\odot\sqrt{1 - |U_{e1}|^2}, \quad \text{IH spectrum (B)}. \tag{19}$$

The mixing matrix element of U constrained by the CHOOZ and Palo Verde data is now $|U_{e1}|^2$:

$$|U_{e1}|^2 = \sin^2\theta, \quad \text{IH spectrum (B)}. \tag{20}$$

We would like to emphasize that Eqs. (9) and (10) are valid in the two conventions for the ordering of the neutrino masses discussed above.

A few comments are in order. The $\bar{\nu}_e$ survival probability depends only on the four continuous parameters $\Delta m^2_\odot$, $\sin^2\theta_\odot$, $\Delta m^2_{\rm atm}$, $\sin^2\theta$, and on a single "discrete" parameter—the type of the neutrino mass spectrum—NH or IH. The terms in the second lines of Eq. (9) and Eq. (10) are responsible for the dominant effects in the survival probability for the intermediate baseline experiment under consideration in the case of the high LMA solution of the solar neutrino problem. The study of the dominant oscillations can thus constrain the solar neutrino oscillation parameters. While the terms in the first lines of Eq. (9) and Eq. (10) give the subdominant, faster oscillations driven by $\Delta m^2_{\rm atm}$, the terms in the last lines are responsible for the difference between the probabilities corresponding to the NH and IH neutrino mass spectra. The detection of this subleading oscillatory behavior would be an indication of the nonvanishing of the mixing angle θ in the PMNS matrix U. It will also enable the experiment under discussion to determine $\Delta m^2_{\rm atm}$ with a high precision. Finally, for sufficiently large values of $\sin^2\theta$ it should, in principle, be possible to distinguish the normal from the inverted hierarchy spectrum. Let us stress that the difference of the survival probabilities for the NH and the IH spectra lies in the interference term: the existing solar neutrino and KamLAND data indicate that $\theta_\odot$ is not maximal so that $\sin\theta_\odot \neq \cos\theta_\odot$.

One can rewrite the term in parenthesis in the last line of Eq. (9) and Eq. (10) in the form

$$\cos\left(\frac{\Delta m^2_{\rm atm} L}{2E_\nu} - \frac{\Delta m^2_\odot L}{2E_\nu}\right) - \cos\frac{\Delta m^2_{\rm atm} L}{2E_\nu} = 2\sin\frac{\Delta m^2_\odot L}{4E_\nu}\sin\left(\frac{\Delta m^2_{\rm atm} L}{2E_\nu} - \frac{\Delta m^2_\odot L}{4E_\nu}\right). \tag{21}$$

Thus, it consists of an oscillating function, with approximately the same frequency as the $\Delta m^2_{\rm atm}$-driven oscillations, modulated with a period which is twice the period of the usual $\Delta m^2_\odot$-driven oscillations. In particular, the amplitude of this term is the maximal possible at values of L/E_ν where the survival probability goes to its $\Delta m^2_\odot$-induced minima, and vanishes at its local maxima.

III. THE EXPERIMENT

Antineutrinos from nuclear reactor sources are detected through their inverse β-decay reaction with protons in the detector. The visible energy $E_{\rm vis}$ of the emitted positron is

TABLE I. Number of events in the case of absence of $\overline{\nu}_e$ oscillations for the different reactor experimental setups considered in this paper.

Power P (GW)	Threshold E_{th} (MeV)	Baseline L (km)	Exposure T (kTy)	No osc Events
5	1.0	20	3	14971
5	2.6	20	3	10585
5	1.0	30	3	6654
5	2.6	30	3	4704
25	1.0	20	3	74855
25	1.0	30	3	33269

related to the energy of the incoming antineutrino E_ν and to the masses of the proton, neutron and positron as

$$E_{\rm vis} \equiv E_\nu + m_{e^+} - (m_n - m_p) \simeq E_\nu - 0.78 \ \ \text{MeV}. \tag{22}$$

The $E_{\rm vis}$ spectrum of detected events in the no oscillation case, which takes into account the initial spectrum of antineutrinos emitted by the reactor and the inverse β-decay cross section, has a bell-shaped distribution, centered at about $E_{\rm vis} \sim 2.8$ MeV. The total number of expected events for the no oscillation case is given in Table I. We consider a single reactor plant with power of either 5 GW (achievable, e.g., at Heilbronn, Germany [31]) or 25 GW (achievable at Kashiwazaki, Japan), as the only relevant source of neutrinos, neglecting the possible contaminations due to other plants at larger distances. We also assume that the reactors have a 100% efficiency. It is trivial to adapt our results to a given reactor efficiency. We present our results as function of the product of the exposure time and the active mass of the detector. We will assume for this product values in the range 3–5 kT y and consider baselines 20–30 km. The total statistics depends on $\mathcal{L} = PM\ T$, the product of the reactor power (P), the detector mass (M) and time of exposure (T), thus we express our results in units of GWkTy. Since the neutrino flux decreases as the inverse square of the baseline length, the shorter baselines obviously have much more statistics than the longer ones. We assume a liquid scintillation detector similar to ones used in the other reactor experiments like CHOOZ and KamLAND. We assume 8.48×10^{31} free protons per kton of detector mass as in KamLAND [6]. We use an energy resolution of $\sigma(E)/E = 5\%/\sqrt{E}$, E in MeV for "our" detector, assuming some improvement with respect to KamLAND, which reported a $\sigma(E)/E = 7.5\%/\sqrt{E}$ [6].

In Table I we present the number of no oscillation events for two different visible energy thresholds of 1.0 MeV and 2.6 MeV. While at higher energies the spectrum is known with relatively high accuracy, at lower energies a possible contamination from geophysical neutrinos and from the time variation of fuel composition is expected [37]. The KamLAND experiment puts a conservative lower threshold of $E_{\rm vis} > 2.6$ MeV [6] to avoid the error associated with the geophysical neutrinos. However, since the reactor flux is the highest around 2.8 MeV, it is desirable to include these parts of the energy spectrum to increase the statistical power of the experiment. We note from Table I that the number of observed events goes up by a factor of 1.4 when the effective threshold energy E_{th} is lowered from 2.6 MeV to 1.0 MeV. Further, with a larger energy window to be used in the data analysis, and correspondingly a large interval in L/E_ν, it is possible, in principle, to reconstruct a larger number of $\Delta m^2_{\rm atm}$-driven oscillation periods, and even to detect both the SPMIN and SPMAX connected to the $\Delta m^2_\odot$-driven oscillations. The latter is crucial for the study of sub-leading effects performed in the second part of this paper.

The ratio of the number of events expected from geophysics sources to the total number of antineutrinos detected can be estimated for a given experimental setup. In their first published data [6], KamLAND estimated the number of these spurious events to be 9, while the total data set contained 32 events with energy below the energy cutoff ($E_{th} = 2.6$ MeV) and 54 above this threshold. For KamLAND this ratio therefore comes up to be about 30% below 2.6 MeV. However, the number of background events due to the geophysical neutrinos is quite model dependent and a very good understanding and modeling (see, e.g., [38]) of the energy spectrum of these events would allow one to use the whole data sample in the range (1.0–7.2) MeV, by subtracting the geophysics background from the observed event spectrum, with just an additional source of systematics in the analysis—the extent of the uncertainty depending on the accuracy of the knowledge of the geophysical neutrino background.

The whole e^+-energy spectrum could also be used in a very high statistics experiment with a sufficiently powerful reactor source. The contamination of the data sample from geophysical neutrino background at low energies is proportional to the active mass of the detector. Thus, decrease in the detector volume compensated with an increase in the reactor antineutrino flux, results in a reduction of the fraction of events due to this background. We can determine the flux of $\overline{\nu}_e$ from a reactor in the absence of oscillations as a function of the distance traveled and of the power of the source:

$$\Phi \equiv \frac{P}{L^2}. \tag{23}$$

For KamLAND, summing over all the reactors which contribute (see for instance [39] for a complete listing), one gets

$$\Phi^{\rm Kam} \simeq 3 \times 10^{-3} \ \ \text{GW/km}^2. \tag{24}$$

As a comparison, using three possible choices for the pair (L/km, P/GW) as (30,5), (20,5) and (20,24), one gets for Φ values that are bigger by a factor of 1.5, 4 and 20, respectively. Accordingly, the fraction of background events from the geophysical neutrinos can be reduced by this factor, as a consequence of the larger flux. In particular, for the last case, the geophysical neutrinos contribution would be at the percent level even for a 1 kiloton detector like KamLAND and could be safely accounted for. For lower fluxes and large detectors, either a very accurate subtraction procedure needs to be applied, or it would be necessary to keep the cutoff in

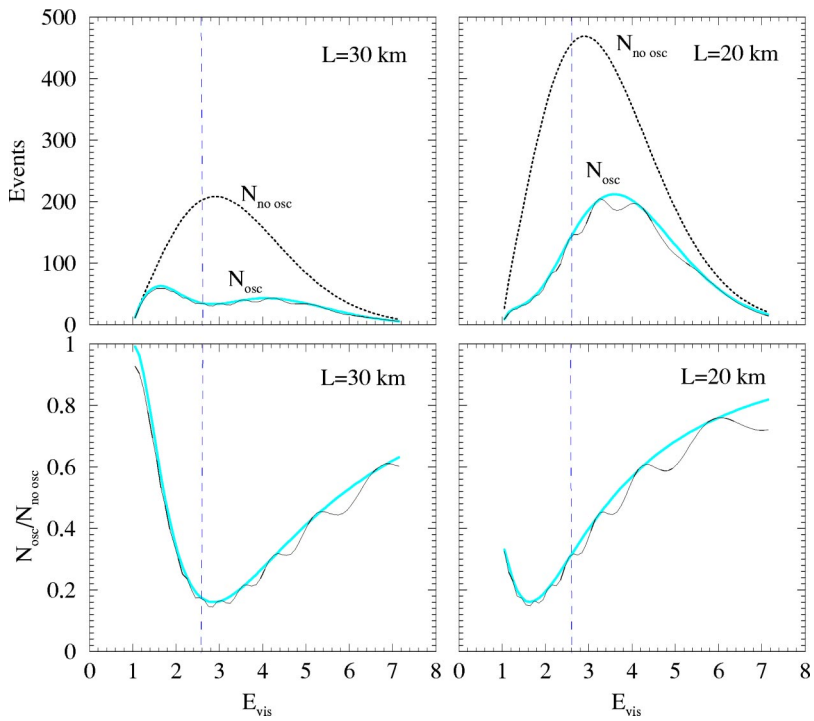

FIG. 1. The observed e^+-energy spectrum (in 0.1 MeV bins) for the 20 km (right panel) and 30 km (left panel) experiment with reactor power 5 GW and exposure of 3 kTy (15 GWkTy). The dotted black lines in the top panels give the number of events in the absence of oscillations. The solid lines give the events for $\bar{\nu}_e$ oscillations with $\Delta m^2_{\odot}=1.5\times10^{-4}$ eV^2, $\sin^2\theta_{\odot}=0.3$, and $\Delta m^2_{\rm atm}=2.5\times10^{-3}$ eV^2. The solid gray line corresponds to the spectrum for $\sin^2\theta=0.0$, while the solid black line shows the spectrum for $\sin^2\theta=0.03$. The bottom panels show the corresponding ratio of events in the cases of $\bar{\nu}_e$ oscillations and of absence of oscillations for the two values of $\sin^2\theta$. The event spectra in the case of $\bar{\nu}_e$ oscillations are for neutrino mass spectrum with normal hierarchy.

the low energy part of the spectrum as in KamLAND. In this paper we neglect throughout the contribution coming from geophysical neutrinos—we either put an energy threshold of 2.6 MeV, or when we lower E_{th} to 1.0 MeV we assume that either they can be accounted for, or they can be safely neglected.

Backgrounds may also result from radioactive impurities and from cosmic ray interactions. However, these can be effectively suppressed in realistic experiments [31] and we completely neglect backgrounds in this paper.

In presence of neutrino oscillation, the detected energy spectrum at a distance L from the reactor is obtained by convoluting the survival probability given by Eq. (9) or Eq. (10) with the spectrum obtained with no oscillation. This leads to a suppression of the number of detected events, and to a distortion of the energy spectrum itself, whose dependence on the parameters entering the survival probabilities may be used to extract them through a χ^2 fit of the data.

The optimal distance in order to resolve the first minimum (SPMIN) of the survival probability, and extract with good accuracy a measurement of $\Delta m^2_{\odot}$ and $\sin^2\theta_{\odot}$, according to Eq. (9) and Eq. (10), is given by[6]

$$L^*\equiv\frac{2\pi E_\nu}{\Delta m^2_{\odot}}, \tag{25}$$

so that its choice depends on the actual value of $\Delta m^2_{\odot}$ and on the typical energy involved. If E_ν is at the peak of the spectrum (3.5–4 MeV), this choice implies a maximal depletion of the total number of events. We will consider always the case in which a relatively large statistics is accumulated, so that the main source of information is the differential energy spectrum of detected events. In this case a large window of different energies can be used to determine L^*. However, as long as the baseline of the experiment is large enough to include the first oscillation minimum (SPMIN) in the interval of energies used for the measurements, preferably in the part of the energy spectrum with highest statistics, the experiment is expected to display a good sensitivity to the solar neutrino oscillation parameters.

We show in Fig. 1 the spectrum of observed events for two specific baselines of 20 km and 30 km for reactor power of 5 GW and 3 kTy exposure. We note that the 30 km experiment has much less events than the 20 km experiment. The solid lines in the bottom panels show that the SPMIN for the 30 km experiment comes around 2.8 MeV, where the flux is the highest. For the 20 km experiment the SPMIN comes at around 1.6 MeV. Correspondingly, if the lower energy cutoff is set to $E_{th}=2.6$ MeV (shown by the dashed lines in Fig. 1), the 20 km experiment would miss the SPMIN. Therefore for the 20 km experiment, the E_{th} has to be lowered to below 1.6 MeV if the value of $\Delta m^2_{\odot}$ happens to be 1.5×10^{-4} eV^2. For higher values of $\Delta m^2_{\odot}$, the SPMIN will shift to higher energies and the threshold could be taken higher: for $\Delta m^2_{\odot}=2.5\times10^{-4}$ eV^2, for instance, SPMIN is at $E_{\rm vis}=3.2$ (5.3) MeV for $L=20$ (30) km.

Figure 1 also shows the "subdominant" oscillation effects dependent on $\Delta m^2_{\rm atm}$ and $\sin^2\theta$, imprinted on the large dominant oscillation wave driven by the solar neutrino oscillation parameters. The experiment could be expected to have sensitivity to the parameters $\Delta m^2_{\rm atm}$ and $\sin^2\theta$, driving the subdominant oscillations, if the energy resolution of the detector

[6]This distance is also the optimal one for enhancing the effect of the interference term in the survival probability distinguishing the NH and IH spectrum cases, as seen from Eq. (21), because for these values of L/E_ν the modulation of the beating-like term is maximal.

would be good enough to enable a large statistics experiment like the one we consider here, to break the total number of events into fine energy bins. In particular, to resolve the oscillatory behavior one needs bins much smaller than the oscillation period

$$\Delta E \ll \Delta E^* \equiv \frac{4\pi E_\nu^2}{\Delta m^2 L}, \tag{26}$$

where Δm^2 is the relevant neutrino mass squared difference driving the oscillations. This implies that for a given L, higher energy resolution and smaller bins are required in order to resolve effects due to a larger mass squared difference. As a numerical example,

$$\Delta m^2_\odot = 1.5\times 10^{-4}\ \text{eV}^2 \Rightarrow \Delta E^*_\odot = 7.1\ \text{MeV},$$

$$\Delta m^2_{\text{atm}} = 2.7\times 10^{-3}\ \text{eV}^2 \Rightarrow \Delta E^*_{\text{atm}} = 0.4\ \text{MeV},$$

for energies at the peak of the spectrum ($E_\nu = 3.6$ MeV) and at the distance $L = 30$ km. It is clear that energy bins with a width of 0.425 MeV (as in KamLAND) allow a good reconstruction of the spectral distortion due to $\Delta m^2_\odot$-driven oscillations, but would average out completely the subleading Δm^2_{atm} effects. Using as a guide rule the assumption that to resolve an oscillation one needs $\Delta E_{\text{vis}} \lesssim \Delta E^*/4$, the reconstruction of Δm^2_{atm}-driven oscillations requires to use energy bins having width of ~ 0.1 MeV. The use of shorter distances can soften this problem, as Eq. (26) indicates. However, with an energy resolution of $\sigma(E)/E = 5\%/\sqrt{E}$, it should be possible to have bins of the size of 0.1 MeV, at least as long as the energy is not very large. We will show that with bins of 0.1 MeV width, and $L = 20$ km, one can improve on the CHOOZ limit for $\sin^2\theta$, and if $\sin^2\theta$ is found to be large enough to be detectable in this experiment, Δm^2_{atm} can be determined with a very high precision.

With an experimental setup which allows a sufficiently small bin size and large enough statistics to measure the subdominant oscillations, one can hope to gain information about the neutrino mass hierarchy using the last interference terms in Eq. (9) and Eq. (10).

Finally, one has to take into account the presence of systematic errors both in the determination of the flux normalization and in the energy calibration of the detector. The KamLAND collaboration estimated a total systematic uncertainty of about 6.42% in their first published analysis [6]. The bulk of this error comes from uncertainty in the overall flux normalization. The use of a near detector can improve this flux normalization error to as low as 0.8% [31]. The error on energy calibration could be taken as 0.5% [41]. We use a total systematic uncertainty of 2%, and we discuss in detail the effect of varying this uncertainty in the analysis which follows.

IV. PRECISION NEUTRINO OSCILLATION PHYSICS: $\Delta M^2_\odot$ AND $\sin^2 2\theta_\odot$ IN THE HIGH LMA REGION

In this section we study quantitatively the precision measurements of the solar neutrino oscillation parameters $\Delta m^2_\odot$ and $\sin^2\theta_\odot$, possible in the intermediate baseline reactor experiment discussed in the previous section under the assumption that $\Delta m^2_\odot$ lies in the high LMA region. We simulate the "data" at certain plausible values of $\Delta m^2_\odot$ and $\sin^2\theta_\odot$ and obtain allowed regions in the parameter space from a dedicated χ^2 analysis. For the errors we assume a Gaussian distribution and define our χ^2 as

$$\chi^2 = \sum_{i,j} (N_i^{data} - N_i^{theory})(\sigma_{ij}^2)^{-1}(N_j^{data} - N_j^{theory}), \tag{27}$$

where N_i^α ($\alpha = data, theory$) is the number of events in the ith bin, σ_{ij}^2 is the covariant error matrix containing the statistical and systematic errors and the sum is over all bins. We compare the sensitivities obtained for two possible baselines, 20 km and 30 km. To quantify the sensitivity we define the relative precision p_a for a certain parameter a at a given C.L. as

$$p_a = \frac{a_{max} - a_{min}}{a_{max} + a_{min}}, \tag{28}$$

where a_{max} (a_{min}) are the maximal (minimal) allowed value of a found at the chosen C.L. We check quantitatively the impact of (1) the energy threshold E_{th}, (2) bin size ΔE and (3) systematic uncertainties. We also study the impact of increasing the statistics by a factor of 5.

As has been noted earlier in the context of KamLAND [40], the sensitivity to $\sin^2\theta_\odot$ can be reduced considerably by the uncertainty in the parameter $\sin^2\theta$. We therefore analyze first the impact this uncertainty can have on the precision of $\sin^2\theta_\odot$ determination in the intermediate baseline reactor experiment of interest. Since the baseline is optimized to measure predominantly the $\Delta m^2_\odot$-driven oscillations, we assume that the Δm^2_{atm}-driven oscillations are averaged out. This corresponds to the realistic case of using a sufficiently large e^+-energy bin size. The expression for the survival probability would then reduce to

$$P_{ee} \approx \cos^4\theta \left(1 - \sin^2 2\theta_\odot \sin^2 \frac{\Delta m^2_\odot L}{4E_\nu}\right), \tag{29}$$

where we have neglected the term $\sim \sin^4\theta$. Therefore the uncertainty in $\sin^2\theta$ essentially brings up to a $\sim 10\%$ uncertainty in the $\bar{\nu}_e$ survival probability. Since the factor $\cos^4\theta$ can only reduce the survival probability, it does not affect the upper limit on the allowed range of $\sin^2\theta_\odot$. However, it can have an effect on the lower limit on $\sin^2\theta_\odot$ reducing it further, and thus can worsen, in principle, the precision of the experiment. Using Eq. (29) we get approximately for the *additional* error on $\sin^2 2\theta_\odot$ due to the uncertainty in the value of $\sin^2\theta$

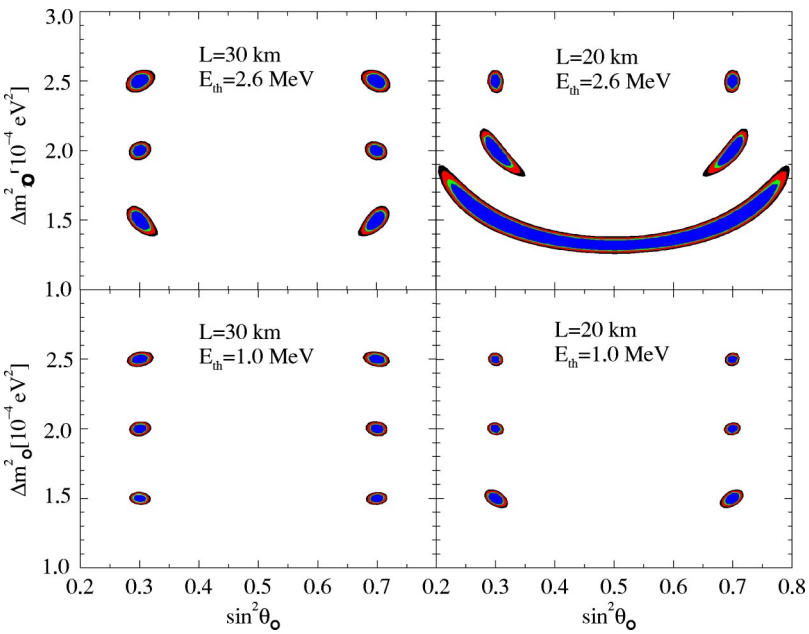

FIG. 2. Simulated two parameter fit of the e^+-energy spectrum in the $\Delta m^2_\odot - \sin^2\theta_\odot$ plane. We assume $\sin^2\theta=0$, $\sin^2\theta_\odot=0.3$ and vary the value of $\Delta m^2_\odot$. We compare results at $L=20$ km and $L=30$ km, with the lower cutoff on the energy spectrum at $E_{th}=2.6$ MeV and at $E_{th}=1.0$ MeV. The energy bin size is chosen as $\Delta E=0.425$ MeV, systematic uncertainties are taken as 2% and the statistics correspond to 15 GWkTy. Shown are the 90%, 95%, 99% and 99.73% (3σ) C.L. contours.

$$\delta(\sin^2 2\theta_\odot) \approx \frac{2\Delta P_{ee}\sin^2\theta}{\sin^2\dfrac{\Delta m^2_\odot L}{4E_\nu}} + 2\frac{\left(1-\sin^2 2\theta_\odot \sin^2\dfrac{\Delta m^2_\odot L}{4E_\nu}\right)\Delta(\sin^2\theta)}{\sin^2\dfrac{\Delta m^2_\odot L}{4E_\nu}}, \tag{30}$$

where ΔP_{ee} and $\Delta(\sin^2\theta)$ are the uncertainties in the determination of the survival probability and $\sin^2\theta$, respectively. We work in a scenario in which one would use the SPMIN in order to determine $\sin^2 2\theta_\odot$. In the SPMIN region one has $\sin^2(\Delta m^2_\odot L/4E_\nu)\sim 1$ and therefore

$$\delta(\sin^2 2\theta_\odot) \approx 2\Delta P_{ee}\sin^2\theta + 2\cos^2 2\theta_\odot \Delta(\sin^2\theta). \tag{31}$$

Thus, in this SPMIN scenario, the first term gives an extra contribution of about $2\Delta P_{ee}\sin^2\theta$ *to the allowed range of* $\sin^2 2\theta_\odot$. Since, as we will see in the present section, in the experiment under consideration the allowed range of $\Delta P_{ee} \lesssim 0.1$ even under the most conservative conditions, this term gives an extra contribution to the allowed range which is $\lesssim 0.01$. The second term is independent of the precision of a given experiment (i.e., on ΔP_{ee}) and depends only on the best-fit value of $\cos^2 2\theta_\odot$ and on the error in $\sin^2\theta$. For the current 3σ error in $\sin^2\theta$ of 0.05 and best-fit $\cos^2 2\theta_\odot$ of 0.16, this would give an increase of only 0.018. The suppression of this term is mainly due to the presence of the factor $\cos^2 2\theta_\odot$ which is a relatively small number for the current best-fit solution. Thus, even though the uncertainty in $\sin^2\theta$ brings a 10% uncertainty in the value of P_{ee}, it increases the allowed range of $\sin^2 2\theta_\odot$ only by $\lesssim(2-3)\%$, if one uses the SPMIN region for the $\sin^2 2\theta_\odot$ determination.

The error in the measured value of $\sin^2 2\theta_\odot$ due to the uncertainty in the value of $\sin^2\theta$ is considerably larger in an experiment like KamLAND, which is sensitive primarily to the region of the maximum of the $\overline{\nu}_e$ survival probability[7] (SPMAX). In this case the oscillatory term $\sin^2(\Delta m^2_\odot L/4E_\nu) \neq 1$ and can be quite small, so that the extra contribution to the uncertainty in $\sin^2 2\theta_\odot$, given roughly by Eq. (30), would be rather large. The first term in the expression in the right-hand side of Eq. (30) becomes relatively large due to the presence of the oscillatory term in the denominator and the second term becomes even larger due to the presence of the same term both in the denominator and in the numerator. Thus, for KamLAND the impact of the uncertainty in $\sin^2\theta$ on $\sin^2\theta_\odot$ determination is essentially related to the fact that the $\Delta m^2_\odot$-dependent oscillatory term for KamLAND is relatively small, resulting in rather big contributions from both terms in Eq. (30). This explains the relatively large effect of the $\sin^2\theta$ uncertainty on the $\sin^2 2\theta_\odot$ determination noticed in [40]. We assert that to reduce the impact of the $\sin^2\theta$ uncertainty on the determination of $\sin^2\theta_\odot$, one needs to "tune" the experiment to the SPMIN. This observation gives further credence to our statement that the best experimental setup for determining the solar neutrino mixing angle with high precision is a reactor experiment sensitive to the SPMIN.

In Figs. 2 and 3 we show the regions of allowed values of $\Delta m^2_\odot$ and $\sin^2\theta_\odot$, obtained with "data" simulated at various values of $\Delta m^2_\odot > 1.0\times 10^{-4}$ eV^2 and $\sin^2\theta_\odot=0.3$. We assume a statistics corresponding to an exposure of 15 GWkTy (5GW$\times$3kTy) [31], bin size $\Delta E=0.425$ MeV and plausible systematic uncertainty of 2%. Figure 2 shows the allowed regions obtained for $\sin^2\theta=0$, corresponding to the case of 2-neutrino $\Delta m^2_\odot$- driven oscillations. In Fig. 3 we display the

[7]This is valid both for $\Delta m^2_\odot \sim 7.2\times 10^{-5}$ eV^2 and for $\Delta m^2_\odot \sim 1.5\times 10^{-4}$ eV^2.

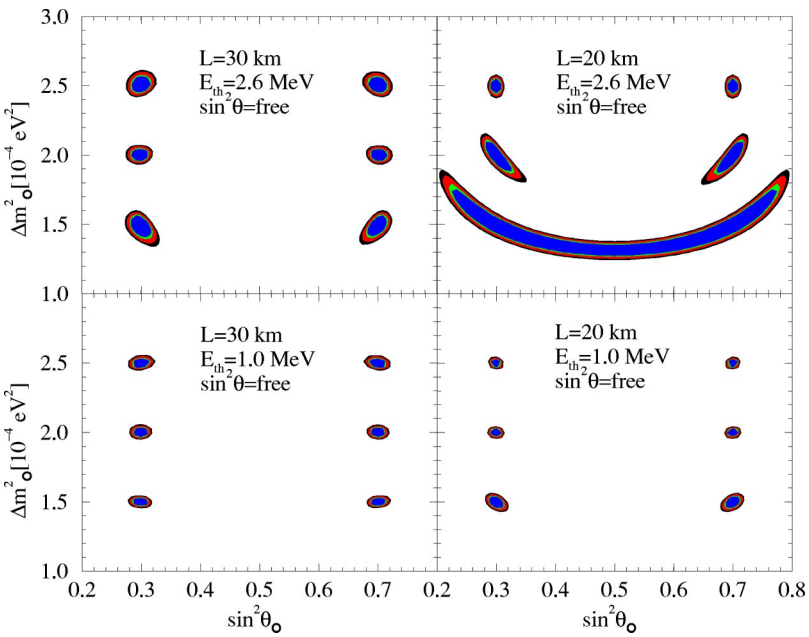

FIG. 3. The same as in Fig. 2 but for $\sin^2\theta$ allowed to vary freely within its 99.73% C.L. allowed range, $\sin^2\theta<0.05$.

corresponding allowed regions in a complete 3-neutrino mixing scheme with $\sin^2\theta$ allowed to vary freely within the 99.73% C.L. allowed range, $\sin^2\theta<0.05$. As a comparison of the two figures indicates, the effect of keeping $\sin^2\theta$ free, on the allowed ranges of the solar neutrino oscillation parameters in general, and on $\sin^2\theta_\odot$ in particular, is rather small. This is compatible with the conclusions of the analysis presented above. Since the effect of keeping $\sin^2\theta$ free is small, in the rest of this section we neglect the uncertainty due to $\sin^2\theta$ on the precision of the $\Delta m^2_\odot$ and $\sin^2\theta_\odot$ determination.

In Fig. 2 we compare the precision obtained on the solar neutrino oscillation parameters for two intermediate baselines of 20 km and 30 km, with and without imposing the low energy cutoff of 2.6 MeV.[8] For the baseline of $L=30$ km, depending on the "true" values of the parameters, at 99% C.L. a precision respectively of (6–7)% and (3–6)% is possible to achieve for $\sin^2\theta_\odot$ and $\Delta m^2_\odot$ even with $E_{th}=2.6$ MeV. These errors reduce only slightly to (5–6)% and $\sim 2\%$, respectively, when the threshold is lowered to 1.0 MeV, owing mainly to the fact that the statistics increases, but also to the fact that the SPMIN is fully used in the measurement.

For the $L=20$ km experiment on the other hand, the precision for both $\Delta m^2_\odot$ and $\sin^2\theta_\odot$ (and especially for $\sin^2\theta_\odot$) is relatively low if the effective threshold of $E_{th}=2.6$ MeV is applied, and if $\Delta m^2_\odot=1.5\times10^{-4}$ eV^2. As discussed in the previous section, for larger values of $\Delta m^2_\odot$ which produce the SPMIN at $E_{\rm vis}>2.6$ MeV, it is still possible to reach high precision in the determination of $\sin^2\theta_\odot$ and $\Delta m^2_\odot$ even with the cutoff of $E_{th}=2.6$ MeV. These values are somewhat disfavored by the current data [11–13]. If the threshold is lowered to 1.0 MeV, the experiment can "see" the full SPMIN even for $\Delta m^2_\odot=1.5\times10^{-4}$ eV^2 and the sensitivity to both $\Delta m^2_\odot$ and $\sin^2\theta_\odot$ becomes remarkable. The $\Delta m^2_\odot$ can be determined with a $\sim 2\%$ precision, while the $\sin^2\theta_\odot$ would be known to within $\sim(3-4)\%$, at the 99% C.L. With $E_{th}=1.0$ MeV even though both $L=20$ km and $L=30$ km baseline experiments would be sensitive to SPMIN, the precision of the shorter baseline experiment is higher, owing to the larger statistics expected.

We have studied the effect of using smaller bins in the e^+-energy spectrum. As explained in the previous section, there is no substantial improvement in the precision of the fit to the solar neutrino oscillation parameters $\Delta m^2_\odot$ and $\sin^2\theta_\odot$ with this strategy. The binning energy used by KamLAND ($\Delta E=0.425$ MeV) is already sufficient and one does not need to use smaller bins. However, we will see in the next sections that a better energy resolution could allow for the extraction of other information embedded in the subdominant oscillations.

One of the crucial issues in these types of experiments is thought to be the control of the systematic error. Indeed, a large systematic uncertainty on the energy spectrum could threaten to wash out the possibility of extracting any information from the data. In Fig. 4 we show the impact of the systematic uncertainty on the expected precision. The plots show the allowed areas obtained assuming 1% and 3% systematic uncertainties and can be compared with the lower panels in Fig. 2, where the systematic uncertainty is taken as 2%. By comparing the relative precision on the parameters, we note that while the precision on $\Delta m^2_\odot$ remains essentially unaffected by the exact value of the systematic uncertainty if the latter does not exceed $\sim 4\%$, the precision of $\sin^2\theta_\odot$ may show a very mild dependence, the error in $\sin^2\theta_\odot$ obviously decreasing with the reduction in the systematic error. However, the impact is not large (see also [29] where the performance of KamLAND is studied under assumption of various anticipated systematic errors). This implies that, at least for

[8]For all the cases we get two solutions in $\sin^2\theta_\odot$, the real one and a "fake" one on the "dark side" ($\sin^2\theta_\odot>0.5$). This fake "dark-side" solutions are ruled out by the solar neutrino data. Nonetheless we show them in our plots for the sake of completeness.

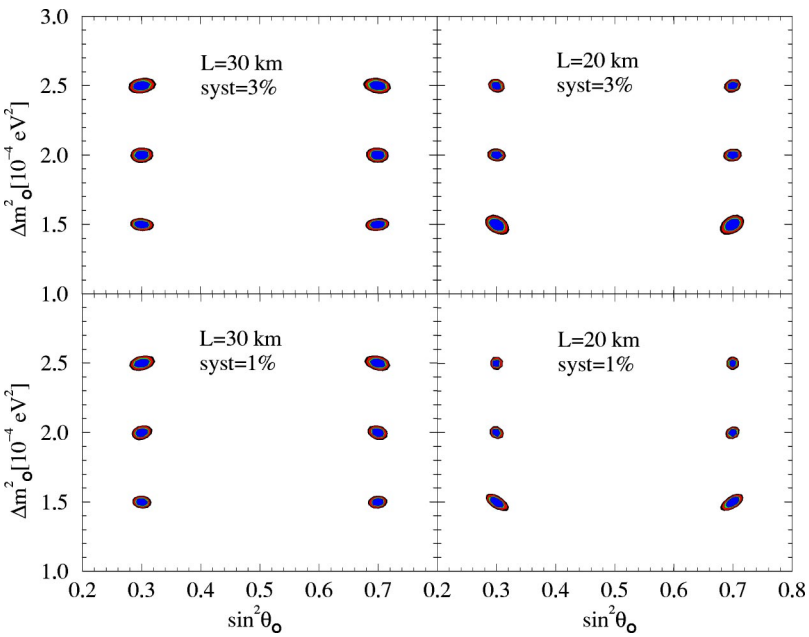

FIG. 4. The same as the lower panels in Fig. 2 but showing the effect of varying the systematic error.

reasonably small values of the systematic uncertainties, their impact on the precision of the parameter determination is only marginal. This result is essentially due to the fact that we are assuming rather large statistics, allowing for a good reconstruction of the oscillatory pattern in the energy spectrum. Similar conclusions were recently drawn in the context of a short baseline experiment at nuclear reactors ($L=1.7$ km) in [41].

By contrast, the precision of $\Delta m^2_\odot$ and $\sin^2\theta_\odot$ measurement can be increased if we increase the statistics, say 5 fold. This could be done using a reactor complex of total power comparable to the Kashiwazaki site (24.3 GW) and a large enough detector. We note that the error in the statistical determination of both $\Delta m^2_\odot$ and $\sin^2\theta_\odot$ would go down below the percent level. With this statistics even the effect of the systematic uncertainty on the precision determination of the parameters is expected to be low and one can achieve remarkable accuracy.

V. PRECISION PHYSICS FROM $\Delta M^2_{\rm atm}$-DRIVEN (SUBDOMINANT) OSCILLATIONS

In this section we will consider the setup where the experiment could be sensitive to the $\Delta m^2_{\rm atm}$-driven subdominant oscillations. As discussed in Sec. III, one has to use relatively small energy bins in order to observe these oscillation effects. We first consider the potential of the intermediate baseline reactor experiment of interest in improving the bound on $\sin^2\theta$. We next assume that $\sin^2\theta$ is sufficiently large and can therefore lead to observable $\Delta m^2_{\rm atm}$-driven oscillations and investigate under what conditions one can use these "fast" oscillations to determine $\Delta m^2_{\rm atm}$ with a high precision. Finally, we study the possibility of achieving what is probably a most ambitious goal—to get information on the neutrino mass hierarchy by observing the reactor $\overline{\nu}_e$ oscillations at intermediate baselines.

A. Improving the limit on $\sin^2\theta$

We investigate in what follows the impact of several experimental conditions on the achievable sensitivity on $\sin^2\theta$. We show in Fig. 5 the $\sin^2\theta$ sensitivity obtainable in a 15 GWkTy statistics experiment. We generate the "data" at $\sin^2\theta=0$ and at each value of $\sin^2\theta$ we plot the difference between the χ^2 function obtained at that value of $\sin^2\theta$ and the χ^2_{min}, which obviously comes at $\sin^2\theta=0$. We define the 3σ and 90% C.L. limit levels as $\Delta\chi^2=9$ and 2.71, respectively, corresponding to a one parameter fit.

The sensitivity to $\sin^2\theta$ increases substantially if the baseline L is reduced. It follows from Eq. (25) that the best sensitivity to $\sin^2\theta$ is achieved for $L=$ few km [41,42]. The intermediate baselines we are considering are not optimized for the measurement of θ. The sensitivity to $\sin^2\theta$ of the experiment under discussion is worse than that of the experiment proposed recently in [41,42] with a distance of 1.7 km. Still, the experiment with $L=20$ km, would allow to put an upper bound of

$$\sin^2\theta < 0.021\ (0.012), \tag{32}$$

at the 3σ (90%) C.L. (Fig. 5, top left panel), which is a noticeable improvement over the current 3σ bound of $\sin^2\theta < 0.05$.

Rather relevant for the sensitivity to $\sin^2\theta$, in addition to the distance L, is the width of the final state e^+ energy bins. As could be expected, the smaller bins give a better sensitivity to the value of $\sin^2\theta$. Bins with width of 0.1 MeV give a 50% improvement in sensitivity compared to the case of bin width of 0.425 MeV. Another relevant factor is the presence of a low energy cutoff in the part of the spectrum used in the fit: the sensitivity improves with the inclusion of the lower energy data by, e.g., changing the cutoff energy from 2.6 MeV to 1.0 MeV. Finally, the last panel in Fig. 5 illustrates the effect of the systematic uncertainties on the sensitivity to $\sin^2\theta$. As discussed in detail in the previous section, the sys-

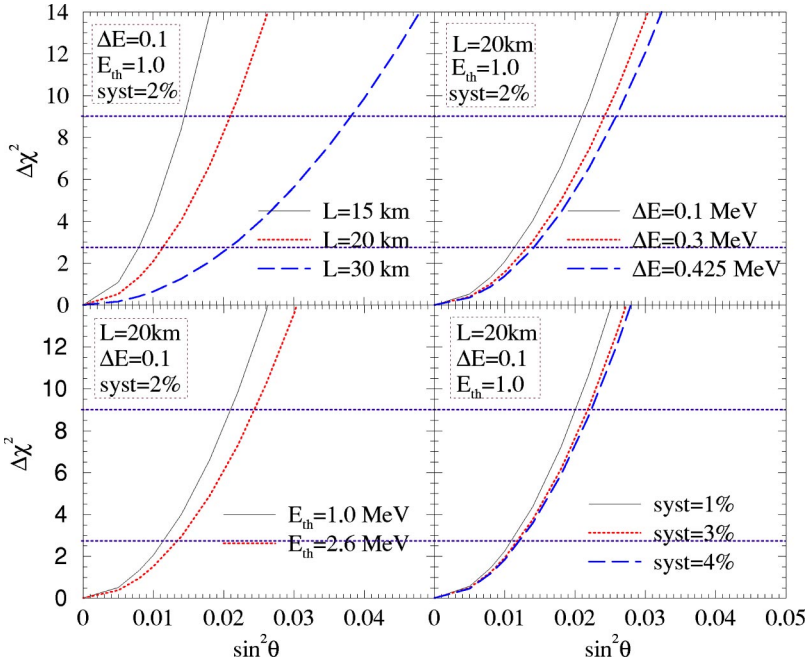

FIG. 5. Study of the sensitivity to $\sin^2\theta$. Shown are the $\Delta\chi^2$ obtained as a function of $\sin^2\theta$, when fitting a simulated "data" set generated for $\sin^2\theta=0$, $\Delta m^2_{\rm atm}=2.5\times10^{-3}$ eV^2, $\Delta m^2_{\rm atm}=1.5\times10^{-4}$ eV^2 and $\sin^2\theta_\odot=0.3$. For a particular value of $\sin^2\theta$, the other parameters are allowed to vary freely in the fit. The two horizontal lines correspond to 3σ and 90% C.L., respectively. We assume a total exposure of $\mathcal{L}=15$ GWkTy, and explore the impact of the baseline (L), width of energy bins (ΔE), the systematic uncertainties and the application of a low-energy cutoff (E_{th}) on the $\sin^2\theta$ sensitivity.

tematic error in the $\sin^2\theta$ measurement has a small but non-negligible effect—the limit improving marginally with the reduction of the error.

We show in Fig. 6 the $\sin^2\theta$ sensitivity when the statistics are increased by a factor of five: we consider statistics corresponding to 75 GWkTy. Clearly, the increase in statistics improves the $\sin^2\theta$ sensitivity and at 3σ (90% C.L.) limit for the $L=20$ baseline case reads (Fig. 6, top left panel)

$$\sin^2\theta<0.01\ \ (0.0055). \tag{33}$$

Thus, for these very high statistics we get a sensitivity to $\sin^2\theta$ which is almost of the same order as that expected to be reached in the "Reactor-I" experiment discussed in [41]. Note that with the increase of the statistics, the effect of both the systematic error and of the value of E_{th} chosen on the $\sin^2\theta$ sensitivity decreases. The decreasing of the energy bin size, however, has essentially the same effect of increasing the sensitivity.

B. Measuring $\Delta m^2_{\rm atm}$ and $\sin^2\theta$

The experimental setup we consider is optimized for extremely precise measurement of $\theta_\odot$, $\Delta m^2_\odot$, and for distinguishing which hierarchy is realized in the neutrino mass spectrum (as we will see in the next section), provided the high-LMA solution is the correct one. Nevertheless, in order to achieve these goals, a relatively large statistics and a suf-

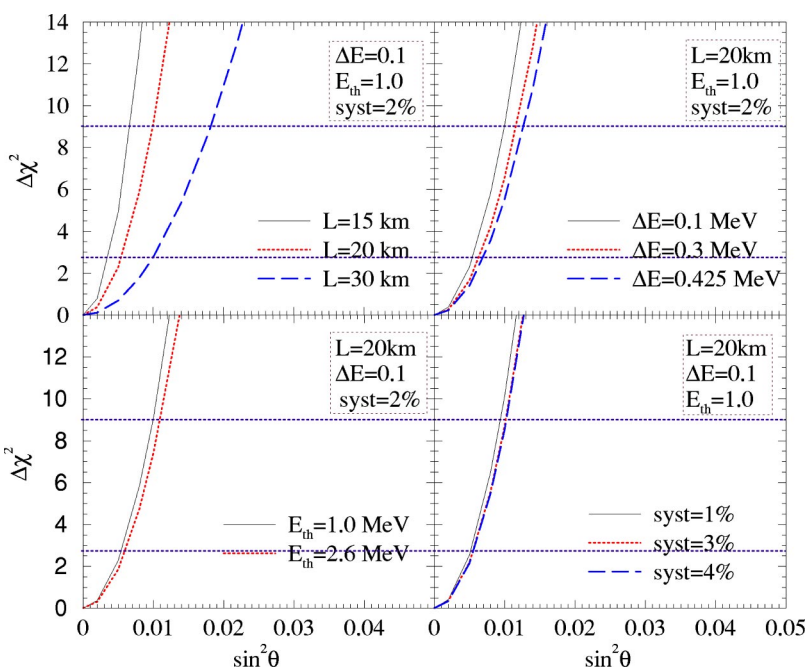

FIG. 6. The same as in Fig. 5, but with statistics increased by a factor of five ($\mathcal{L}=75$ GWkTy).

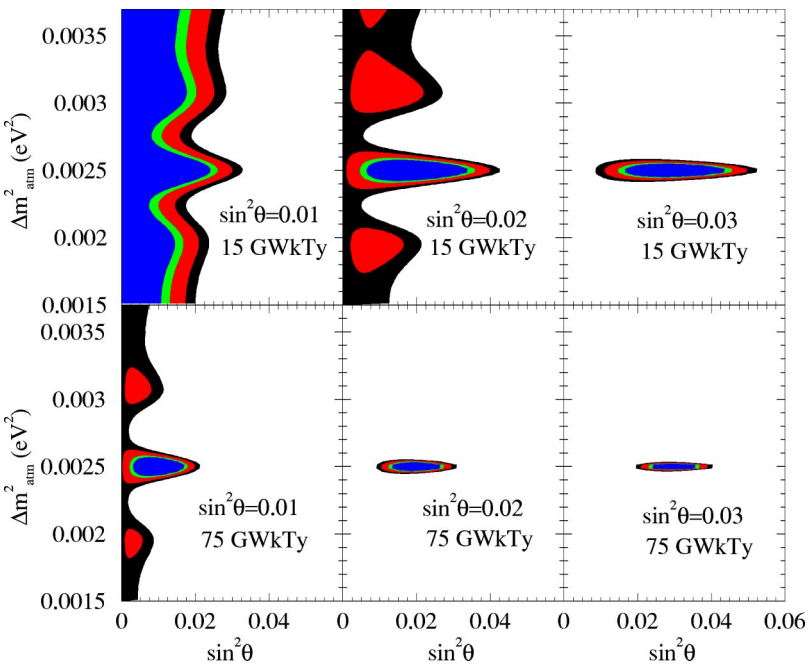

FIG. 7. The 90%, 95%, 99% and 99.73% C.L. allowed regions obtained by fitting "data" set simulated at $\Delta m^2_{\rm atm}=2.5\times10^{-3}$ eV^2 and three different "true" values of $\sin^2\theta$. The solar parameters $\Delta m^2_{\odot}$ and $\sin^2\theta_{\odot}$ are taken to be 1.5×10^{-4} eV^2 and 0.3, respectively. The statistics assumed corresponds to $\mathcal{L}=15$ GWkTy for the upper panels and to $\mathcal{L}=75$ GWkTy for the lower panels. The distance used is $L=20$ km. The bin size is taken as 0.1 MeV, the lower energy cutoff is $E_{th}=1.0$ MeV, and the systematic uncertainty is assumed to be 2%. Both the "data" set and the fitted e^+ spectrum correspond to NH neutrino mass spectrum.

ficiently good energy resolution are required. With these favorable conditions fulfilled and bin width of 0.1 MeV, one could hope to improve on the precision of $\Delta m^2_{\rm atm}$ and $\sin^2\theta$, provided $\sin^2\theta$ is nonzero and is sufficiently large. *We have checked that both of these measurements are rather independent of the value of* $\Delta m^2_{\odot}$, *so that they could be performed in this type of an experiment even if the low-LMA solution is confirmed by the KamLAND Collaboration.*

In Fig. 7 we show the allowed regions in the $\Delta m^2_{\rm atm}$-$\sin^2\theta$ plane, obtained for $L=20$ km and two different statistics samples: the top panels correspond to 15 GWkTy, while the lower panels are for a 75 GWkTy exposure. The results shown in Fig. 7 are for three different "true" values of $\sin^2\theta$ and for $\Delta m^2_{\rm atm}=2.5\times10^{-3}$ eV^2, assuming this to be the "true" value. Similar results for $\Delta m^2_{\rm atm}=2.0\times10^{-3}$ eV^2 and the same three values of $\sin^2\theta$ are presented in Fig. 8. We take a systematic uncertainty of 2% and consider 0.1 MeV bins spanning the entire visible energy spectrum between (1.0–7.2) MeV. In these figures we keep $\Delta m^2_{\odot}$ and $\sin^2\theta_{\odot}$ fixed at 1.5×10^{-4} eV^2 and 0.3, respectively. Since, as we have shown in the previous section, the intermediate baseline experiment itself will restrict the allowed values of $\Delta m^2_{\odot}$ and $\sin^2\theta_{\odot}$ to within a few percent of their "true" value, our results remain practically unchanged even if these parameters were allowed to vary freely in the analysis. As Fig. 7 demonstrates, in the 15 (75) GWkTy case the experiment

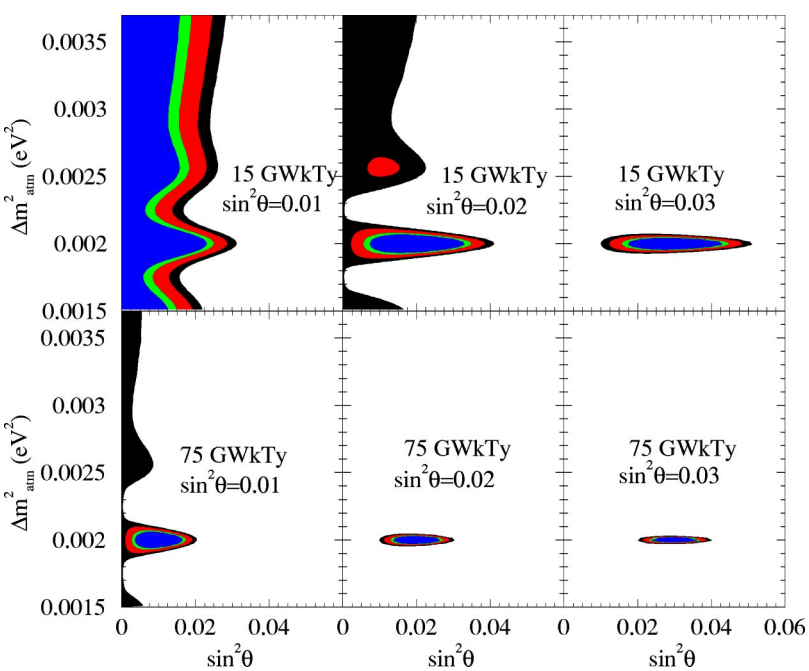

FIG. 8. The same as in Fig. 7, but assuming that the "true" value of $\Delta m^2_{\rm atm}=2\times10^{-3}$ eV^2.

under discussion has almost no sensitivity to the value of $\Delta m^2_{\rm atm}$ if $\sin^2\theta \lesssim 0.02$ (0.01). Note the similarity between these limiting values of $\sin^2\theta$ and the limit on $\sin^2\theta$ which the 15 (75) GWkTy experiment can provide if the "true" value of $\sin^2\theta$ is 0, given in the previous subsection. This implies that below the indicated respective limiting values of $\sin^2\theta$, the experiment we are discussing cannot distinguish between a zero and a nonzero $\sin^2\theta$ and thus fails to "see" the $\Delta m^2_{\rm atm}$-driven oscillations. The reason for the modest sensitivity to $\sin^2\theta$ is related to the fact that the L is chosen for "our" experiment to be sensitive to the SPMIN, caused by the $\Delta m^2_{\odot}$-driven oscillations. Therefore L is much bigger than the L^* [cf. Eq. (25)] which corresponds to the SPMIN associated with the oscillations due to $\Delta m^2_{\rm atm}$. The lack of accuracy in the reconstruction of the details of a single oscillation period (in $E_{\rm vis}$) affects strongly the sensitivity to $\sin^2\theta$ which controls the amplitude of the oscillations. However, this should not affect the sensitivity to $\Delta m^2_{\rm atm}$, which determines the oscillation length, because of the presence of many oscillation periods in the relatively large energy window offered by the spectrum itself.

Thus, if $\sin^2\theta$ is large enough so that the $\Delta m^2_{\rm atm}$-driven oscillations can be observed in the experiment under discussion, $\Delta m^2_{\rm atm}$ can be measured with a high precision. Indeed, in the case when the "true" value of $\sin^2\theta = 0.03$, $\Delta m^2_{\rm atm}$ can be determined to within a few percent accuracy at the 99% C.L. This accuracy could be comparable to the sensitivity of the JPARC (JHF-SK) project to $\Delta m^2_{\rm atm}$[9] [43]. It is certainly much better than the sensitivity to $\Delta m^2_{\rm atm}$ of the $L = 1.7$ km short baseline experiments [41] with the same statistics. This is somewhat unexpected since the $L = 1.7$ km experiment is optimized to see the $\Delta m^2_{\rm atm}$-driven oscillations. However, one should keep in mind that the $L = 1.7$ km baseline experiment cannot constrain the solar neutrino oscillation parameters. The uncertainty in $\Delta m^2_{\odot}$[10] allows $\Delta m^2_{\odot}$ to take on values as high as $(2-3)\times 10^{-4}$ eV^2. This drastically reduces the sensitivity of the $L = 1.7$ km experiment to $\Delta m^2_{\rm atm}$. In the experimental setup we are discussing, the solar parameters are determined to a very high degree of accuracy by the experiment itself and no external input on their errors is required. Thus, the intermediate baseline experiment has a better sensitivity to $\Delta m^2_{\rm atm}$, provided $\sin^2\theta$ is sufficiently large, while the sensitivity to $\sin^2\theta$ of the shorter baseline experiment is better for the reasons discussed above.

Finally, we have verified that even if the low-LMA solution is confirmed as the true solution of the solar neutrino problem, the intermediate baseline experiment could still be used to measure $\Delta m^2_{\rm atm}$ and/or constrain $\sin^2\theta$.

We stress that Figs. 7 and 8 are obtained using Eq. (9), i.e., assuming that the neutrino mass spectrum conforms to a NH. Our conclusions for the sensitivity to $\sin^2\theta$ and $\Delta m^2_{\rm atm}$ would remain the same for the case of IH mass spectrum. For a given "data" set, the allowed region in the parameter space, especially the fitted values of $\Delta m^2_{\rm atm}$, depend on the hierarchy assumed if the $\Delta m^2_{\odot}$ is in the high-LMA region. The possibility of two types of neutrino mass hierarchy leads to an ambiguity in the allowed values of $\Delta m^2_{\rm atm}$ obtained, as we will show in the next subsection. However, even though the assumption of the "wrong" hierarchy can lead to another (separated) allowed region in the parameter space, it does not describe the data so well as the "correct" hierarchy and is disfavored, in general. This can be used to gain insight into the type of hierarchy the neutrino mass spectrum has and can allow "our" intermediate baseline experiment to determine the hierarchy.

Let us stress that the question of the hierarchy becomes relevant if $\Delta m^2_{\odot}$ lies in the high LMA zone. This will be the subject of our discussion in the next subsection. If the true solution turns out to be low LMA, the last terms in Eq. (9) and Eq. (10) would be negligible and sensitivity to hierarchy would be lost. Let us emphasize, however, that even in this case it would still be possible to improve the existing limits on $\sin^2\theta$, and—if $\sin^2\theta$ is sufficiently large—to measure $\Delta m^2_{\rm atm}$ with an exceptional precision.

C. Normal vs inverted hierarchy

The next question that may be answered with the experiment under discussion is whether the neutrino mass spectrum is with normal hierarchy or with inverted hierarchy. As pointed out in Sec. III and follows from Eq. (21), the baseline $L = 20$–30 km is particularly suited for that purpose. In this subsection we present results for $L = 20$ km. We use the highest statistics and smallest energy bins and consider the entire visible energy spectrum with a low energy cutoff of $E_{th} = 1.0$ MeV. We assume also that the "true" value of $\sin^2\theta$ is nonzero and is sufficiently large. As it follows from Eq. (9) and Eq. (10), the predictions for the final state e^+-spectrum distortions in the NH and IH cases differ only if the solar neutrino mixing angle $\theta_{\odot} \neq \pi/4$. Maximal mixing is currently disfavored by the solar neutrino and KamLAND data [11–13]. We use the current best-fit value for the solar neutrino mixing angle, corresponding to $\sin^2\theta_{\odot} = 0.3$. The value of $\sin^2\theta_{\odot}$ will be measured with a very high precision in the reactor experiment under discussion itself.

In Fig. 9 we show the visible energy spectrum expected for both the NH and IH cases. The left-hand panel shows the number of events, while the right-hand panel shows the ratio of the number of events in the case of $\bar{\nu}_e$ oscillation ("oscillation events") to the number of events in the absence of oscillations ("no oscillation events"). The thick gray line is for the case of $\Delta m^2_{\rm atm} = 2.5\times 10^{-3}$ eV^2 and NH, the dotted line corresponds to $\Delta m^2_{\rm atm} = 2.5\times 10^{-3}$ eV^2 and IH, while the thin solid line is for $\Delta m^2_{\rm atm} = 2.6\times 10^{-3}$ eV^2 and IH. Thus, for the same value of $\Delta m^2_{\rm atm}$, the e^+-spectrum deformations expected for NH and IH are different owing to the last terms in Eq. (9) and Eq. (10). One might expect on the basis of Eqs. (9) and (10) that the IH e^+ spectrum would fit

[9]The experiment we are discussing has a much larger statistics than the planned JPARC (JHF-SK) experiment; for the precise determination of $\Delta m^2_{\rm atm}$ it also requires $\sin^2\theta$ to be sufficiently large.

[10]For this uncertainty the authors of [41] have used the current 3σ uncertainty on $\Delta m^2_{\odot}$, found in the combined solar neutrino and KamLAND data analysis.

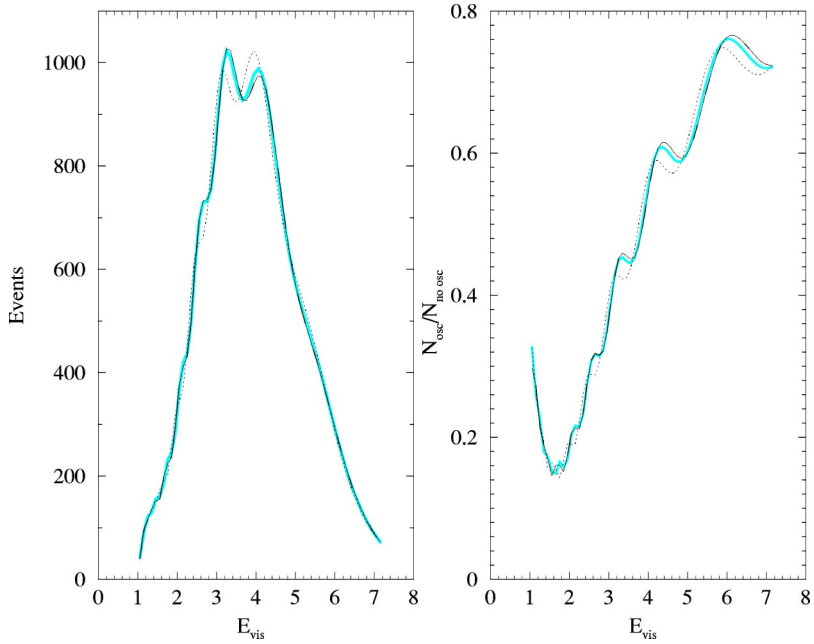

FIG. 9. The energy spectrum (in 0.1 MeV bins) of the events in the case of $\bar{\nu}_e$ oscillations (left panel), and the ratio of events in the cases of oscillations and absence of oscillations (right panel), showing the effect of hierarchy for an $L=20$ km experiment. The thick gray line corresponds to the case for NH with $\Delta m^2_{\rm atm}=2.5\times10^{-3}$ eV^2 while the dotted and thin solid line correspond to the case of IH with $\Delta m^2_{\rm atm}=2.5\times10^{-3}$ eV^2 and $\Delta m^2_{\rm atm}=2.6\times10^{-3}$ eV^2, respectively. The statistics assumed is $\mathcal{L}=75$ GWkTy, while $\sin^2\theta=0.03$, $\Delta m^2_{\odot}=1.5\times10^{-4}$ eV^2 and $\sin^2\theta_{\odot}=0.3$.

a NH e^+ spectrum with a value of $\Delta m^2_{\rm atm}$ that is larger than the "true" value by a range which would be of the order of $\Delta m^2_{\odot}$. If the experiment has a sensitivity to $\Delta m^2_{\rm atm}$ which is better than, or is at least of the same order as $\Delta m^2_{\odot}$, one might expect two nondegenerate solutions in the $\Delta m^2_{\rm atm}$-$\sin^2\theta$ parameter space for the same data set: one for NH and another for IH.

However, *we would like to stress that even though the IH e^+ spectrum could approximately reproduce the NH e^+ spectrum, it cannot exactly reproduce the latter. Hence, if the NH is the true hierarchy, the case of IH mass spectrum would always be disfavored by the data from "our" experiment compared to the NH spectrum*. We have seen in the previous section that the experimental setup we are discussing could have a very high sensitivity to $\Delta m^2_{\rm atm}$, and therefore we can expect the large statistics intermediate baseline reactor experiments to determine the type of neutrino mass hierarchy, for sufficiently large $\sin^2\theta$ at least, if the high LMA solution holds.

In Fig. 10 we explicitly show the allowed regions obtained using a "data" set generated in the NH case and fitted by both the NH and IH expressions for the $\bar{\nu}_e$ survival probability. The results shown are obtained using the 75 GWkTy statistics and a higher 125 GWkTy statistics. The "true" value of $\Delta m^2_{\rm atm}$ assumed is 2.5×10^{-3} eV^2, while "true" $\sin^2\theta=0.02$. For the 75 GWkTy case, the two regions overlap at the 3σ level, while for 125 GWkTy they are completely nondegenerate. Note also that for the 125 GWkTy

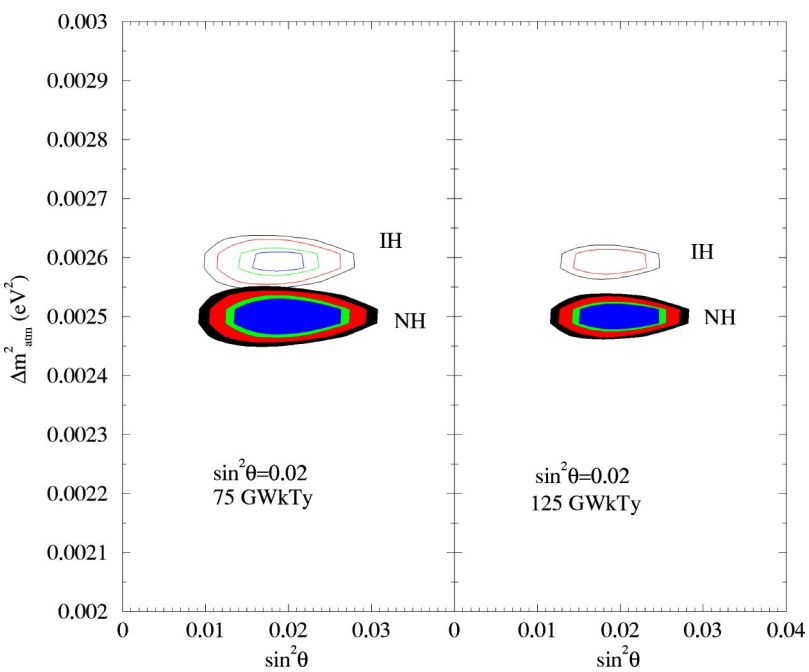

FIG. 10. The same as in Fig. 7, but probing the type of the neutrino mass hierarchy. The "data" sets simulated correspond to NH. The filled contours show the C.L. allowed regions obtained by fitting for the parameters assuming NH. The empty contours show the 90%, 95%, 99% and 99.73% solution regions, obtained by fitting the NH "data" with an IH theory. The contours for the IH are obtained with respect to the χ^2 minima found in the case of the NH. The statistics assumed in the left-hand panel is $\mathcal{L}=75$ GWkTy, while that in the right-hand panel is $\mathcal{L}=125$ GWkTy. We note that while for the $\mathcal{L}=75$ GWkTy case the "wrong" hierarchy is allowed even at the 90% C.L., with the $\mathcal{L}=125$ GWkTy statistics the experiment can rule out the IH at least at the 95% C.L.

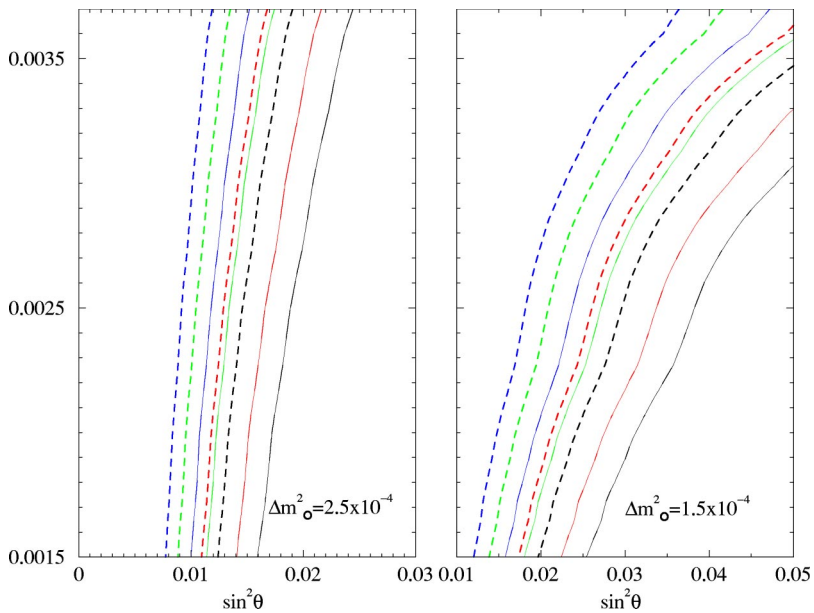

FIG. 11. Contours of constant 99.73%, 99%, 95% and 90% C.L. (from right to left) showing the ability of the $L=20$ km baseline experiment to determine the correct hierarchy at each "true" point in the $\Delta m^2_{\rm atm}-\sin^2\theta$ plane. The solid lines (dashed lines) correspond to $\mathcal{L}=75$ GWkTy ($\mathcal{L}=125$ GWkTy). The results shown are for $\sin^2\theta_\odot=0.30$, and for $\Delta m^2_\odot=1.5\times10^{-4}$ eV^2 (right panel) and $\Delta m^2_\odot=2.5\times10^{-4}$ eV^2 (left panel). For the values of $\Delta m^2_{\rm atm}$ and $\sin^2\theta$, corresponding to points on the plane, located to the right of a given C.L. line, the experiment can rule out the "wrong" hierarchy at that C.L. See the text for further details.

case, the "data" generated for NH spectrum can "rule out" the IH spectrum, at least at the 95% C.L.

In Fig. 11 we show the dependence of the hierarchy sensitivity of the $L=20$ km reactor experiment on the "true" values of $\Delta m^2_{\rm atm}$, $\sin^2\theta$ and $\Delta m^2_\odot$. For each point in the $\Delta m^2_{\rm atm}$-$\sin^2\theta$ parameter space and a given $\Delta m^2_\odot$ and $\sin^2\theta_\odot$, we simulate the observed e^+-energy spectrum assuming NH to be true. We then fit this "observed" spectrum with both the NH and IH through a χ^2 analysis, allowing the parameters $\Delta m^2_{\rm atm}$ and $\sin^2\theta$ to vary freely around their "true" values. The IH spectrum obviously does not fit the "data" as well as the NH and hence is disfavored. To quantify this sensitivity to hierarchy we calculate the difference (χ^2_{diff}) between the χ^2 for the NH and IH for each point in the parameter space and use the definition $\chi^2_{diff}<\Delta\chi^2$ to find whether IH can be ruled out at a given C.L. The $\Delta\chi^2$ is determined by the C.L. considered and we take the 2-parameter definition for it. We show the lines of the C.L. contours in the $\Delta m^2_{\rm atm}$-$\sin^2\theta$ plane for 2 different values of $\Delta m^2_\odot$ and $\sin^2\theta_\odot=0.3$. All "true" values of the parameters located to the right of a given line could allow the experiment to disfavor the IH spectrum at the corresponding C.L. The solid lines give the sensitivities for 75 GWkTy exposure, while the dashed lines are for a 125 GWkTy data set. The sensitivity to hierarchy is maximal for the smallest allowed values of $\Delta m^2_{\rm atm}$ and for these cases it is possible to rule out IH even for smaller values of $\sin^2\theta$. It becomes increasingly more difficult to distinguish between the two types of neu-

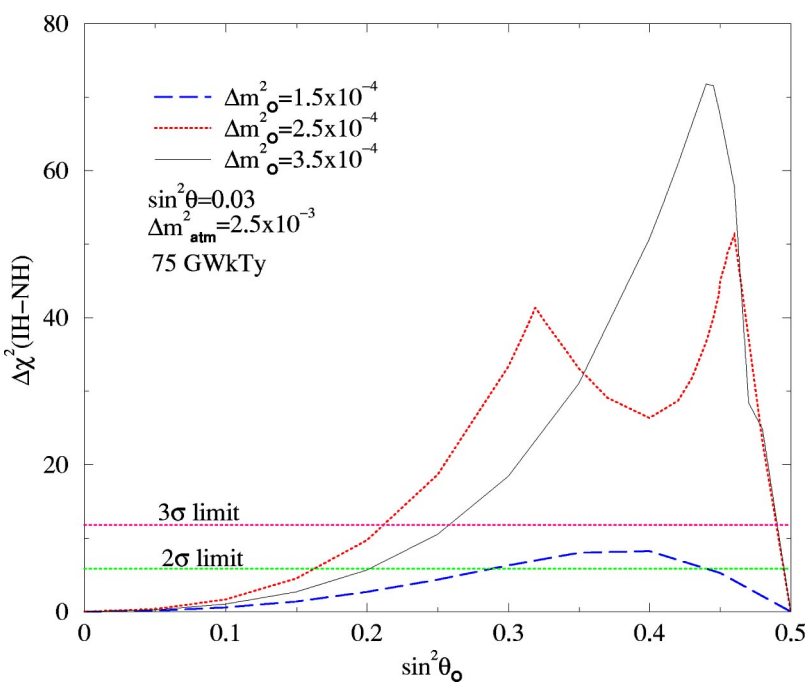

FIG. 12. The difference between the minimal values of χ^2, obtained by fitting a NH "data" set with NH and IH spectrum, as a function of $\sin^2\theta_\odot$. The results shown are for $\Delta m^2_\odot=1.5\times10^{-3}$; 2.5×10^{-3}; 3.5×10^{-3} eV^2. The "true" values of $\Delta m^2_{\rm atm}=2.5\times10^{-3}$ eV^2 and of $\sin^2\theta=0.03$, while the statistics corresponds to $\mathcal{L}=75$ GWkTy.

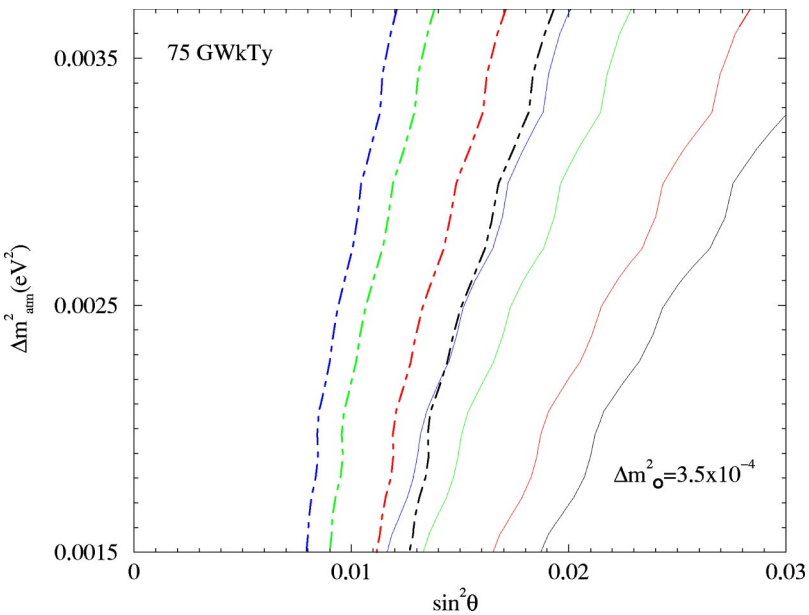

FIG. 13. The same as in Fig.11, for $\mathcal{L}=75$ GWkTy, $\Delta m^2_{\odot}=3.5\times10^{-4}$ eV^2 and two values of $\sin^2\theta_{\odot}$: 0.30 (solid lines) and 0.40 (dash-dotted lines).

trino mass hierarchy as $\Delta m^2_{\rm atm}$ increases, as the figure indicates. The sensitivity of the experiment to hierarchy depends critically on the "true" value of the solar parameters, as is evident from Eq. (9) and Eq. (10). In particular, higher values of $\Delta m^2_{\odot}$ are better suited for hierarchy determination, as can be seen explicitly comparing the two panels in Fig. 11.

The possibility of determining the neutrino mass hierarchy is very sensitive to the value of $\sin^2\theta_{\odot}$. As we have explained above, when we generate the NH "data" and fit them with the IH theory, we allow $\Delta m^2_{\rm atm}$ to vary and take larger values than $\Delta m^2_{\rm atm}$ used to generate the "data." Let us denote the best-fit $\Delta m^2_{\rm atm}$ in the IH case as $\Delta m'^2_{\rm atm}$:

$$\Delta m'^2_{\rm atm}=\Delta m^2_{\rm atm}+\Delta m'^2_{\rm atm}, \tag{34}$$

where $\Delta m^2>0$. The difference between the IH and NH $\overline{\nu_e}$ survival probabilities at each E is given by

$$\begin{aligned}P_{IH}(\overline{\nu_e}\to\overline{\nu_e})-P_{NH}(\overline{\nu_e}\to\overline{\nu_e})=4\sin^2\theta\cos^2\theta\Bigg[&\sin\left(\frac{\Delta m^2_{\rm atm}L}{2E}+\frac{\Delta m^2L}{4E}\right)\sin\left(-\frac{\Delta m^2L}{4E}\right)\\&+\cos^2\theta_{\odot}\sin\left(\frac{\Delta m^2_{\rm atm}L}{2E}+\frac{\Delta m^2L}{2E}-\frac{\Delta m^2_{\odot}L}{4E}\right)\sin\left(\frac{\Delta m^2_{\odot}L}{4E}\right)\\&-\sin^2\theta_{\odot}\sin\left(\frac{\Delta m^2_{\rm atm}L}{2E}-\frac{\Delta m^2_{\odot}L}{4E}\right)\sin\left(\frac{\Delta m^2_{\odot}L}{4E}\right)\Bigg].\end{aligned} \tag{35}$$

When, e.g., $\cos 2\theta_{\odot}=1$, we have $P_{IH}-P_{NH}=0$ for $\Delta m^2=\Delta m^2_{\odot}$. For $\cos 2\theta_{\odot}=0$ (maximal mixing), the difference between the two probabilities is 0 for $\Delta m^2=0$. For the realistic case of $\cos 2\theta_{\odot}\cong(0.10\text{–}0.40)$, it is impossible to have $P_{\rm IH}-P_{\rm NH}=0$ for every value of E from the interval of interest. This is illustrated in Fig. 12, where we show the difference between the minimal values of χ^2 for the "wrong" IH and the "right" NH spectra as a function of $\sin^2\theta_{\odot}$ for "true" $\Delta m^2_{\odot}=1.5\times10^{-4}$; 2.5×10^{-4}; 3.5×10^{-4} eV^2, $\Delta m^2_{\rm atm}=2.5\times10^{-3}$ eV^2 and $\sin^2\theta=0.03$. As Fig. 12 indicates, the best sensitivity to the type of neutrino mass hierarchy is achieved in the interval $\sin^2\theta_{\odot}\cong(0.3\text{-}0.45)$, which is favored by the current solar neutrino and KamLAND data. The rather strong dependence of the sensitivity to the type of neutrino mass hierarchy on $\sin^2\theta_{\odot}$ is illustrated in Fig. 13, in which we show contours of constant C.L. in the $\Delta m^2_{\rm atm}-\sin^2\theta$ plane, at which one could distinguish between the NH and IH spectra, for $\Delta m^2_{\odot}=3.5\times10^{-4}$ eV^2 and $\sin^2\theta_{\odot}=0.30$; 0.40.

One final comment is in order. As Fig. 10 illustrates, for a given "data set" (i.e., "true" value of $\Delta m^2_{\rm atm}$, etc.) and sufficient statistics, the neutrino mass hierarchy ambiguity can lead to two nondegenerate solutions for $\Delta m^2_{\rm atm}$, one for NH and another for IH spectrum. In certain of these cases the intermediate baseline reactor experiment might not be able to rule out the "wrong" hierarchy even at the 90% C.L.

(Fig.10, left panel). However, since the NH and IH give two different and nondegenerate values for $\Delta m^2_{\rm atm}$, in such cases one can use the information from some other very precise experiment, like the proposed JHF-SK or NuMI off-axis experiments with neutrino superbeams [43,44], to determine the correct value of $\Delta m^2_{\rm atm}$. The latter can be used together with the data from the reactor experiment to get information on the hierarchy.

VI. CONCLUSIONS

In this paper we analyzed the physics potential of a reactor neutrino experiment with a relatively large detector at a distance $L\sim 20$–30 km. This distance has been chosen in order to achieve the best sensitivity to the solar neutrino oscillation parameters $\Delta m^2_\odot$ and $\sin^2\theta_\odot$, assuming that the latter lie in the high LMA solution region. We considered the case of three flavor neutrino mixing and used in the analysis the exact expression for the relevant $\bar{\nu}_e$ survival probability. The latter depends, in addition to $\Delta m^2_\odot$ and $\sin^2\theta_\odot$, on $\Delta m^2_{\rm atm}$, driving the atmospheric neutrino oscillations, on θ—the angle limited by the CHOOZ and Palo Verde experiments, and for $\sin^2\theta_\odot<0.50$—on the type of the neutrino mass spectrum which can be with normal hierarchy (NH) or with inverted hierarchy (IH). The current solar neutrino and KamLAND data favor $\sin^2\theta_\odot\sim 0.30$. We discussed strategies and the experimental setup, which would permit to measure $\Delta m^2_\odot$ and $\sin^2\theta_\odot$ with a high precision, get information on (or even measure) $\sin^2\theta$, and if $\sin^2\theta$ is sufficiently large ($\sin^2\theta\gtrsim 0.02$) provide a high precision measurement of $\Delta m^2_{\rm atm}$ and determine the type of the neutrino mass hierarchy. More specifically, we have investigated the impact that (i) the choice of the baseline L, (ii) the effect of using a relatively low e^+-energy cutoff of $E_{th}\sim 1.0$ MeV, (iii) the detector's energy resolution, as well as (iv) the statistical and systematical errors, can have on the measurement of each of the indicated neutrino oscillation parameters.

The precision with which $\Delta m^2_\odot$ and $\sin^2\theta_\odot$ can be determined in the experiment under discussion depends crucially on whether the first $\Delta m^2_\odot$-driven oscillation minimum of the $\bar{\nu}_e$ survival probability falls or not in the interval of e^+ energies which can be used for the measurements in the experiment. For $\Delta m^2_\odot=1.5\times 10^{-4}$ eV^2 (2.5×10^{-4} eV^2) and $L=20$ km, this minimum takes place at the e^+ energy of $E_{vis}=1.6$ (3.2) MeV; for $L=30$ km, it occurs at $E_{vis}=2.8$ (5.3) MeV. This implies that if $\Delta m^2_\odot=1.5\times 10^{-4}$ eV^2, in order to achieve a high precision in the determination of $\Delta m^2_\odot$ and especially of $\sin^2\theta_\odot$ in an experiment with a baseline of $L=20$ km, a relatively low "threshold" energy should be employed, $E_{th}\sim 1.0$ MeV. If, however, $\Delta m^2_\odot\gtrsim 2.0\times 10^{-4}$ eV^2, one can use $E_{th}\cong 2.6$ MeV, as was done in the KamLAND experiment. In the case of $L=30$ km one can use $E_{th}\cong 2.6$ MeV even for $\Delta m^2_\odot\gtrsim 1.5\times 10^{-4}$ eV^2. If the condition under discussion is satisfied, remarkable precision in the measurement of $\Delta m^2_\odot$ and $\sin^2\theta$ can be achieved. For the lower "threshold" energy, $E_{th}\sim 1.0$ MeV, achieving high precision requires a controllable or negligible background due to the geophysical neutrinos in the interval $E_{vis}=(1.0$–$2.6)$ MeV. If a sufficiently accurate modeling of this background is achieved and $E_{th}=1.0$ MeV, assuming $\Delta m^2_\odot=1.5\times 10^{-4}$ eV^2, energy bins of $\Delta E=0.425$ MeV, $\sin^2\theta_\odot=0.3$, 2% systematic error and a total statistics corresponding to $\mathcal{L}=15$ GWkTy, one could determine $\Delta m^2_\odot$ with up to a $\sim 2\%$, and $\sin^2\theta_\odot$ with a 3–4 % uncertainty at 99% C.L. in an experiment with a baseline of $L=20$ km (Figs. 2–4). This impressive results depend rather mildly on the systematic error provided the latter does not exceed $\sim 4\%$ (Fig. 4). The reduction of the e^+-energy bin width leads to a negligible change in the precision with which $\Delta m^2_\odot$ and $\sin^2\theta_\odot$ are measured. The precision can be even higher in the case of a larger statistics.

The same apparatus could be used to extract information on the other parameters entering into the expression for the survival probability, through the study of subleading effects controlled by the (small) mixing angle θ, for which only upper bounds exist at present.

The limit on $\sin^2\theta$ can be lowered to $\sin^2\theta<0.021$ at 99.73% C.L. for $L=20$ km, if the "threshold" energy $E_{th}=1.0$ MeV, the systematic error is 2%, the e^+-energy bin width is $\Delta E=0.1$ MeV and if statistics corresponding to $\mathcal{L}=15$ GWkTy is collected. This result depends strongly on the choice of L: the optimal distance for such a measurement is of a few km, and the shorter the distance with respect to $L=20$ km the stronger this bound would be. The magnitude of e^+-energy bin width and the value of the e^+-energy effective threshold have a considerable impact on the bound as well, while a further reduction of the systematic errors could lead only to a mild improvement. If the statistics is as large as that corresponding to a setup with $\mathcal{L}=75$ GWkTy, one could improve the upper bound to $\sin^2\theta<0.010$ (0.0055) at 99.73% (90%) C.L.

If, on the contrary, a relatively large nonvanishing value of $\sin^2\theta$ is found, the experiment could gain sensitivity to $\Delta m^2_{\rm atm}$ through the detection of the subleading oscillatory properties of the $\bar{\nu}_e$ survival probability. Not averaging out the $\Delta m^2_{\rm atm}$-driven oscillations is crucial for the measurement of $\Delta m^2_{\rm atm}$. This requires a relatively high e^+-energy resolution, permitting a binning in the e^+ energy with a rather small bin width, $\Delta E\cong 0.1$ MeV. Taking $E_{th}=1.0$ MeV and assuming 2% systematic error, we find that a setup with $\mathcal{L}=15$ (75) GWkTy could provide a precise determination of $\Delta m^2_{\rm atm}$ with a few percent uncertainty for $\Delta m^2_{\rm atm}\sim 2.5\times 10^{-3}$ eV^2, if $\sin^2\theta\sim 0.03$ (0.02) (Fig. 7).

Finally, the distance $L=20$ km is the optimal one for distinguishing between the NH and IH neutrino mass spectrum. The relevant $\bar{\nu}_e$ survival probabilities for the two types of spectrum differ for $\sin^2\theta_\odot<0.5$ by a $\sin^2\theta$-suppressed interference term due to the amplitudes of the $\Delta m^2_\odot$- and $\Delta m^2_{\rm atm}$-driven oscillations. For this highly challenging study, a very large statistics is necessary: we considered $\mathcal{L}=75$ and 125 GWkTy. The possibility of distinguishing between the two types of neutrino mass hierarchy was found to depend not only on the values of $\sin^2\theta$ and $\sin^2\theta_\odot$, but also on the values of $\Delta m^2_\odot$ and $\Delta m^2_{\rm atm}$. The dependence on $\Delta m^2_\odot$ and

$\sin^2\theta_\odot$ is particularly strong. For $\Delta m^2_\odot = 1.5\times 10^{-4}$ eV^2, and $\mathcal{L}=75$ (125) GWkTy, one could distinguish the NH from the IH spectrum at 99.73% C.L. in the region of $\Delta m^2_{\rm atm} \lesssim 2.5\times 10^{-3}$ eV^2 if $\sin^2\theta \gtrsim 0.038$ (0.03) (Fig. 11). The type of the neutrino mass spectrum can be determined for considerably smaller values of $\sin^2\theta$ if $\Delta m^2_\odot$ has a larger value (Figs. 12 and 13), or if an even larger statistics would be accumulated. For $\mathcal{L}=75$ GWkTy and $\Delta m^2_\odot = 2.5\times 10^{-4}$ eV^2, for instance, this can be done at 99.73% C.L. for $\sin^2\theta \gtrsim 0.019$ if $\Delta m^2_{\rm atm} \lesssim 2.5\times 10^{-3}$ eV^2 and $\sin^2\theta_\odot = 0.30$ (Fig. 11). As we have shown, the highest sensitivity to the type of the neutrino mass hierarchy is achieved for $\sin^2\theta_\odot \cong (0.30\text{–}0.45)$ (Figs. 12 and 13).

To conclude, the intermediate baseline $L\cong 20$ km reactor neutrino experiments have in the case of the high-LMA solution of the solar neutrino problem a remarkable potential for a high precision measurement of the solar neutrino oscillation parameters $\Delta m^2_\odot$ and $\sin^2\theta_\odot$, which can reduce the error in the values of the latter to a (2–4) %. Such an experiment can also improve the existing bounds on, or measure, $\sin^2\theta$, currently limited by the CHOOZ and Palo Verde data. If $\sin^2\theta$ turns out to be relatively large, $\sin^2\theta \gtrsim 0.02$, the same experiment could measure $\Delta m^2_{\rm atm}$, driving the atmospheric neutrino oscillations, with an error of a few percent and might be able to establish whether the neutrino mass spectrum is with normal or inverted hierarchy.

Note added. The Sudbury Neutrino Observatory (SNO) Collaboration has released data from the salt phase of the experiment very recently [45]. These data when combined with the data from all the other solar neutrino experiments imply $\Delta m^2_\odot \lesssim 2.0\times 10^{-4}$ eV^2 at the 3σ level [46]. This should be compared with the 3σ bound of $\Delta m^2_\odot \lesssim 3.5\times 10^{-4}$ eV^2, obtained using the global solar neutrino data prior to the announcement of the salt phase SNO results [10]. Adding the KamLAND data to the global solar neutrino data further constrains $\Delta m^2_\odot$, and at 3σ the upper bound reads: $\Delta m^2_\odot \lesssim 1.7\times 10^{-4}$ eV^2 [46]. Prior to SNO salt phase results the 3σ bound on $\Delta m^2_\odot$ was somewhat weaker, $\Delta m^2_\odot \lesssim 2.0\times 10^{-4}$ eV^2 [11]. Therefore, the salt enriched data from SNO, when combined with the already existing solar neutrino data, disfavor the high LMA solution, compared to the low LMA solution. However, the high LMA solution cannot be considered as comprehensively ruled out. It is still allowed at the 99.13% C.L. by the combined KamLAND and solar neutrino data [46]. Moreover, the first results from the KamLAND experiment showed only marginal support in favor of the low LMA solution. Therefore the question of whether the high LMA solution is a viable solution of the solar neutrino problem or not can be definitely answered only after a more precise data from the KamLAND experiment will be available. We would also like to stress that the ability of the intermediate baseline experiment to constrain θ_{13} and to determine $\Delta m^2_{\rm atm}$ if θ_{13} is sufficiently large is independent of the true solution of the solar neutrino problem.

ACKNOWLEDGMENTS

S.T.P. would like to thank T. Lasserre for useful discussions and the members of APC Institute at College de France, Paris, and the organizers of the Program on ''Neutrinos: Data, Cosmos and the Planck Scale'' at KITP, Univ. of California at Santa Barbara, where parts of the work on the present study were done, for kind hospitality. M.P. would like to thank R. Shrock and R.G.H. Robertson for useful discussions. S.C. acknowledges help from S. Goswami and A. Bandyopadhyay in developing the computer code used for numerical calculations in the present work, and would like to thank F. Suekane for useful correspondence. This work was supported in part by the Italian MIUR and INFN under the programs ''Fenomenologia delle Interazioni Fondamentali'' and ''Fisica Astroparticellare'' (S.T.P. and S.C.), by the U.S. National Science Foundation under Grant No. PHY99-07949 (S.T.P.) and by the U.S. Department of Energy under contract DE-FG02-92ER-40704 (M.P.).

[1] B.T. Cleveland *et al.*, Astrophys. J. **496**, 505 (1998); SAGE Collaboration, J.N. Abdurashitov *et al.*, Zh. Éksp. Teor. Fiz. **122** 211 (2002) [JETP **95**, 81 (2002)]; GALLEX Collaboration, W. Hampel *et al.*, Phys. Lett. B **447**, 127 (1999); E. Bellotti, talk at Gran Sasso National Laboratories, Italy, 2002; T. Kirsten, talk at Neutrino 2002, XXth International Conference on Neutrino Physics and Astrophysics, Munich, Germany, 2002 (http://neutrino2002.ph.tum.de/).

[2] Super-Kamiokande Collaboration, S. Fukuda *et al.*, Phys. Rev. Lett. **86**, 5656 (2001); Super-Kamiokande Collaboration, S. Fukuda *et al.*, *ibid.* **86**, 5651 (2001).

[3] SNO Collaboration, Q.R. Ahmad *et al.*, Phys. Rev. Lett. **87**, 071301 (2001); SNO Collaboration, Q.R. Ahmad *et al.*, *ibid.* **89**, 011301 (2002).

[4] Super-Kamiokande Collaboration, Y. Fukuda *et al.*, Phys. Rev. Lett. **81**, 1562 (1998); M. Shiozawa, talk given at the Int. Conf. on Neutrino Physics and Astrophysics ''Neutrino'02,'' 2002, Munich, Germany.

[5] K2K Collaboration, M.H. Ahn *et al.*, Phys. Rev. Lett. **90**, 041801 (2003).

[6] KamLAND Collaboration, K. Eguchi *et al.*, Phys. Rev. Lett. **90**, 021802 (2003).

[7] B. Pontecorvo, Zh. Éksp. Teor. Fiz. **53**, 1717 (1967) [Sov. Phys. JETP **26**, 984 (1968)]; S.M. Bilenky and B. Pontecorvo, Phys. Rep. **41**, 225 (1978).

[8] S.M. Bilenky and S.T. Petcov, Rev. Mod. Phys. **59**, 671 (1987).

[9] S.T. Petcov, *Computing Particle Properties*, edited by H. Gausterer and C.B. Lang, Lecture Notes in Physics, Vol. 512 (Springer, Berlin, 1998), p. 281, hep-ph/9806466.

[10] S. Choubey *et al.*, hep-ph/0209222; A. Bandyopadhyay *et al.*, Phys. Lett. B **540**, 14 (2002).

[11] G.L. Fogli *et al.*, Phys. Rev. D **67**, 073002 (2003).

[12] A. Bandyopadhyay *et al.*, Phys. Lett. B **559**, 121 (2003).

[13] M. Maltoni, T. Schwetz, and J.W. Valle, Phys. Rev. D **67**,

093003 (2003); J.N. Bahcall, M.C. Gonzalez-Garcia, and C. Pena-Garay, J. High Energy Phys. **02**, 009 (2003); H. Nunokawa, W.J. Teves, and R. Zukanovich Funchal, Phys. Lett. B **562**, 28 (2003); P. Aliani *et al.*, Phys. Rev. D (to be published), hep-ph/0212212; P.C. de Holanda and A.Y. Smirnov, J. Cosmol. Astropart. Phys. **02**, 001 (2003).

[14] G.L. Fogli *et al.*, Phys. Rev. D **67**, 093006 (2003).

[15] S.M. Bilenky, C. Giunti, and W. Grimus, Prog. Part. Nucl. Phys. **43**, 1 (1999).

[16] B. Pontecorvo, Zh. Eksp. Teor. Fiz. **33**, 549 (1957); **34**, 247 (1958).

[17] Z. Maki, M. Nakagawa, and S. Sakata, Prog. Theor. Phys. **28**, 870 (1962).

[18] S.M. Bilenky *et al.*, Phys. Lett. **94B**, 495 (1980).

[19] M. Doi *et al.*, Phys. Lett. **102B**, 323 (1981).

[20] P. Langacker *et al.*, Nucl. Phys. **B282**, 589 (1987).

[21] CHOOZ Collaboration, M. Apollonio *et al.*, Phys. Lett. B **466**, 415 (1999).

[22] F. Boehm *et al.*, Phys. Rev. Lett. **84**, 3764 (2000); Phys. Rev. D **62**, 072002 (2000).

[23] S.M. Bilenky, D. Nicolo, and S.T. Petcov, Phys. Lett. B **538**, 77 (2002).

[24] A. De Rujula *et al.*, Nucl. Phys. **B168**, 54 (1980).

[25] S.M. Bilenky *et al.*, Phys. Lett. B **356**, 273 (1995).

[26] MINOS Collaboration, D. Michael, talk at the Int. Conf. on Neutrino Physics and Astrophysics ''Neutrino'02,'' 2002, Munich, Germany.

[27] M. Spiro, summary talk at the Int. Conf. on Neutrino Physics and Astrophysics ''Neutrino'02,'' 2002, Munich, Germany.

[28] A. Bandyopadhyay *et al.*, hep-ph/0211266; V.D. Barger, D. Marfatia, and B.P. Wood, Phys. Lett. B **498**, 53 (2001); H. Murayama and A. Pierce, Phys. Rev. D **65**, 013012 (2002).

[29] A. Bandyopadhyay, S. Choubey, and S. Goswami, Phys. Rev. D **67**, 113011 (2003).

[30] S.T. Petcov and M. Piai, Phys. Lett. B **533**, 94 (2002).

[31] S. Schonert, T. Lasserre, and L. Oberauer, Astropart. Phys. **18**, 565 (2003).

[32] S.M. Bilenky *et al.*, Phys. Lett. B **465**, 193 (1999); S.M. Bilenky, S. Pascoli, and S.T. Petcov, Phys. Rev. D **64**, 053010 (2001); S. Pascoli and S.T. Petcov, Phys. Lett. B **544**, 239 (2002); S. Pascoli, S.T. Petcov, and W. Rodejohann, *ibid.* **558**, 141 (2003).

[33] M. Freund *et al.*, Nucl. Phys. **B578**, 27 (2000); see also, e.g., A. De Rujula, M.B. Gavela, and P. Hernandez, *ibid.* **B547**, 21 (1999); V. Barger *et al.*, Phys. Rev. D **62**, 013004 (2000).

[34] V. Barger, D. Marfatia, and K. Whisnant, Phys. Lett. B **560**, 75 (2003); P. Huber, M. Lindner, and W. Winter, Nucl. Phys. **B654**, 3 (2003).

[35] A. Bandyopadhyay, S. Choubey, S. Goswami, and K. Kar, Phys. Rev. D **65**, 073031 (2002).

[36] S.M. Bilenky *et al.*, Phys. Rev. D **54**, 4432 (1996).

[37] V.I. Kopeikin, L.A. Mikaelyan, and V.V. Sinev, Yad. Fiz. **64**, 914 (2001) [Phys. At. Nucl. **64**, 849 (2001)].

[38] G. Fiorentini *et al.*, Phys. Lett. B **558**, 15 (2003).

[39] C. Bemporad, G. Gratta, and P. Vogel, Rev. Mod. Phys. **74**, 297 (2002).

[40] M.C. Gonzalez-Garcia and C. Pena-Garay, Phys. Lett. B **527**, 199 (2002).

[41] P. Huber *et al.*, Nucl. Phys. **B665**, 487 (2003).

[42] H. Minakata *et al.*, Phys. Rev. D **68**, 033017 (2003).

[43] Y. Itow *et al.*, hep-ex/0106019.

[44] D. Ayres *et al.*, hep-ex/0210005.

[45] SNO Collaboration, S.N. Ahmed *et al.*, nucl-ex/0309004.

[46] A. Bandyopadhyay, S. Choubey, S. Goswami, S.T. Petcov, and D.P. Roy, hep-ph/0309174.